7-12-2018

Convex Optimization Approach to the Optimal Power Flow Problem in DC-Microgrids with Energy Storage

Abdullah Mohammed Alzahrani
aa8247@rit.edu

Convex Optimization Approach to the Optimal Power Flow Problem in DC-Microgrids with Energy Storage

By

Abdullah Mohammed Alzahrani

A Thesis Submitted in Partial Fulfillment of the Requirements for the Degree of
Master of Science in Electrical Engineering
Department of Electrical and Microelectronic Engineering
Kate Gleason College of Engineering
Rochester Institute of Technology, Rochester, New York

Supervised By

Dr. Juan Carlos Cockburn
Associate Professor, Department of Computer Engineering

Approved By:

Dr. Juan Carlos Cockburn
Primary Adviser, Department of Computer Engineering

Dr. Luis Carlos Herrera
Secondary Adviser, Department of Electrical Engineering

Dr. Santosh Kurinec
Committee Member, Department of Electrical and Microelectronic Engineering

---

Dr. Panos P. Markopoulos
Committee Member, Department of Electrical Engineering

July 12, 2018

Copyright Warning

ACKNOWLEDGMENT

I would like to give my most sincere gratitude to **Prof. Juan Carlos Cockburn** for his expertise, understanding, patience, and conscientious and kindly guidance during my MSc studies. Thank you very much for offering me the chance to study at Rochester Institute of Technology (RIT), encouraging my research interests and helping me to develop. I appreciate your vast knowledge and skill in many areas, and for taking time to support my thesis work. Your advice and assistance has been invaluable and of great help in getting everything done in a very timely manner.

A very special thanks goes out to **Prof. Luis Carlos Herrera** for giving me precious advice in my research. Your guidance has been extremely valuable for me and will still be helpful for my future career and life. I sincerely appreciate your efforts sharing your knowledge and experience during the research of my thesis.

I must also acknowledge **Prof. Santosh Kurinec** and **Prof. Panos P. Markopoulos**. Thanks for your kind help and support during my MSc studies at RIT.

I would also like to thank my family for the support they provided me through my entire life and during my thesis studies in particular. I would like to take this opportunity to thank my friends for their kind help during my MSc studies. Thanks all of you for bringing me the gorgeous studying atmosphere and assisting me through those extremely tough days.

I would like to thank all the professors and staff members of the Department of Electrical

Engineering, RIT for their extended cooperation and guidance. I also take this opportunity to give thanks to all others who have given me support for the thesis or in other aspects of my study at RIT.

Abstract

Humanity is currently facing a global energy crisis. This is due to the shortage in the conventional energy resources while the demand for energy is rising. In response to this crisis, research in designing more energy efficient systems has gained significant importance. The Microgrids (MGs) are one of the main key elements in giving significant momentum to efficient decentralized energy generation.

From the perspective of MGs power management, economical scheduling for generators, energy storage, and demand loads are critical. Performance optimization processes are needed to minimize the operating costs while considering operational constraints.

In this thesis, the optimal power flow problem for managing energy sources with storage devices is presented for dc microgrids. The power management model has been examined in various scenarios. One of them is based on a network of a six-bus power system, including an energy storage device coupling at a certain bus. The other scenario is based on the same model but including more energy storage devices.

After analyzing the results of these scenarios, several conclusions have been made such as when the energy storage should charge/discharge to minimize costs. The study shows the feasibility of optimal power flow operation in DC microgrids.

Contents

List of Figures

List of Tables

Nomenclature

$\mathcal{N}$	The set of buses
$\mathcal{G}$	The set of generation buses.
$\mathcal{E}$	The set of transmission lines.
$n \sim j$	Buses n and j connected by a line.
H	Denotes hermitian transpose.
$\mathcal{G}$	The graph contains a set $\mathcal{N}$ of nodes and a set $\mathcal{E}$ of edges.
$\mathbb{C}$	The set of Complex numbers.
δ	Voltage phase angles.
$\|V\|$	Voltage magnitudes.
P_n	Active power at bus n.
Q_n	Reactive power at bus n.
V_n	Complex voltage at bus n.
y_{nj}	Admittance of line joining buses n and j.
S_n	The net power injection at bus n.
I_n	The current at bus n.
x	The vector of state variables.
u	The vector of control variables.
$\succeq 0$	Positive Semidefinite
SDP	Semidefinite Program.

SOCP	Second-Order Cone Program.
LP	Linear programming.
QP	Quadratic programming.
NLP	Nonlinear programming.
IPM	Interior point method.
SLP	Sequential Linear Programming.
SM	Simplex Method.
LIM	Lambda-iterative Method.
SQP	Successive Quadratic Programming.
GT	Gradient Techniques.
NT	Newton's Techniques.
KKT	Karush–Kuhn–Tucker.

1 | Introduction

In recent decades, electrical power systems have been significantly changing whereas fixed power generation has been moving towards more distributed generation. The increase in power demand and environmental concerns about conventional power generation are the main reasons for this transformation. An additional critical stimulus is the substantial amount of energy losses in conventional methods. When power is produced from fossil fuels such as coal, hydrocarbons, fuel oil or natural gas, 40%–70% of the energy in the current resources is wasted as heat. Additionally, 2% and 4% is lost in transmission lines and distribution, respectively. Generally, as shown in Fig. 1.2.a, only 33% of the energy input to generation makes it to the user as electricity. Nowadays, distributed generation systems can be placed beside the load to utilize lower capacity of power generation resources, such as renewable energy sources, as seen in Fig. 1.2.b. Solar and wind energy are the most popular types of renewable energy sources that can be integrated into modern power systems and microgrids (MGs) [1, 2], and [3]. Microgrids consist of a collection of such distributed generation systems coordinated with each other in a way that increases the capacity of the system and improves the power quality [4, 5, 6, 7], and [8].

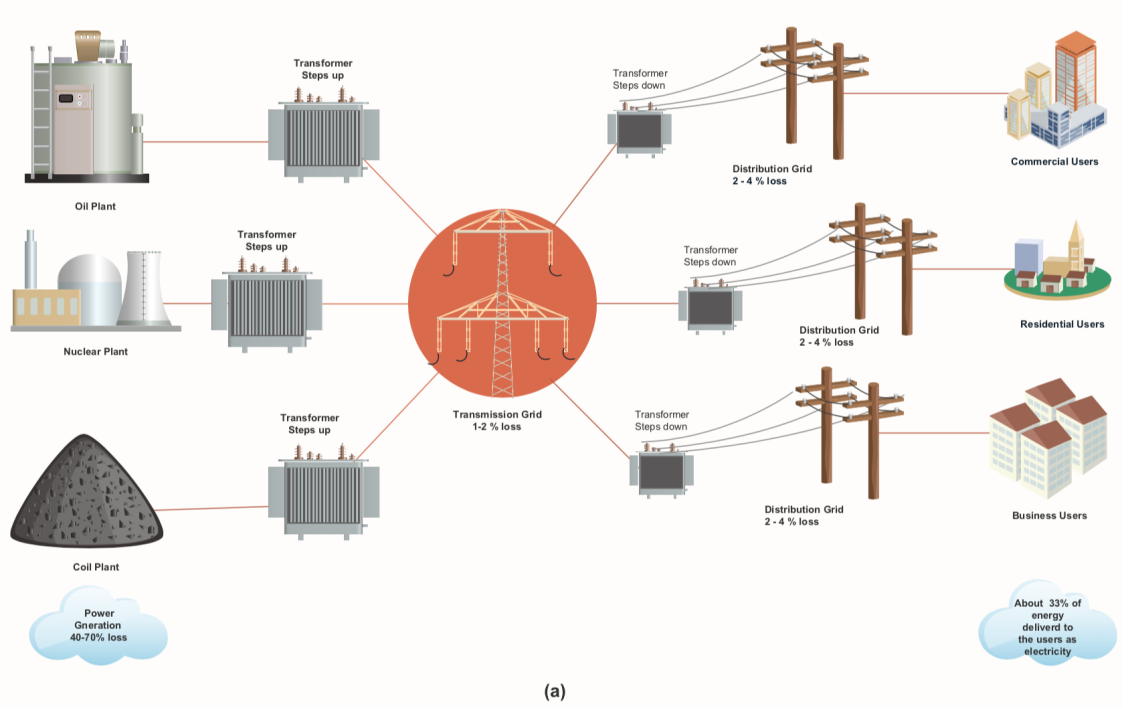

Figure 1.1: (a) Energy losses in traditional power grid

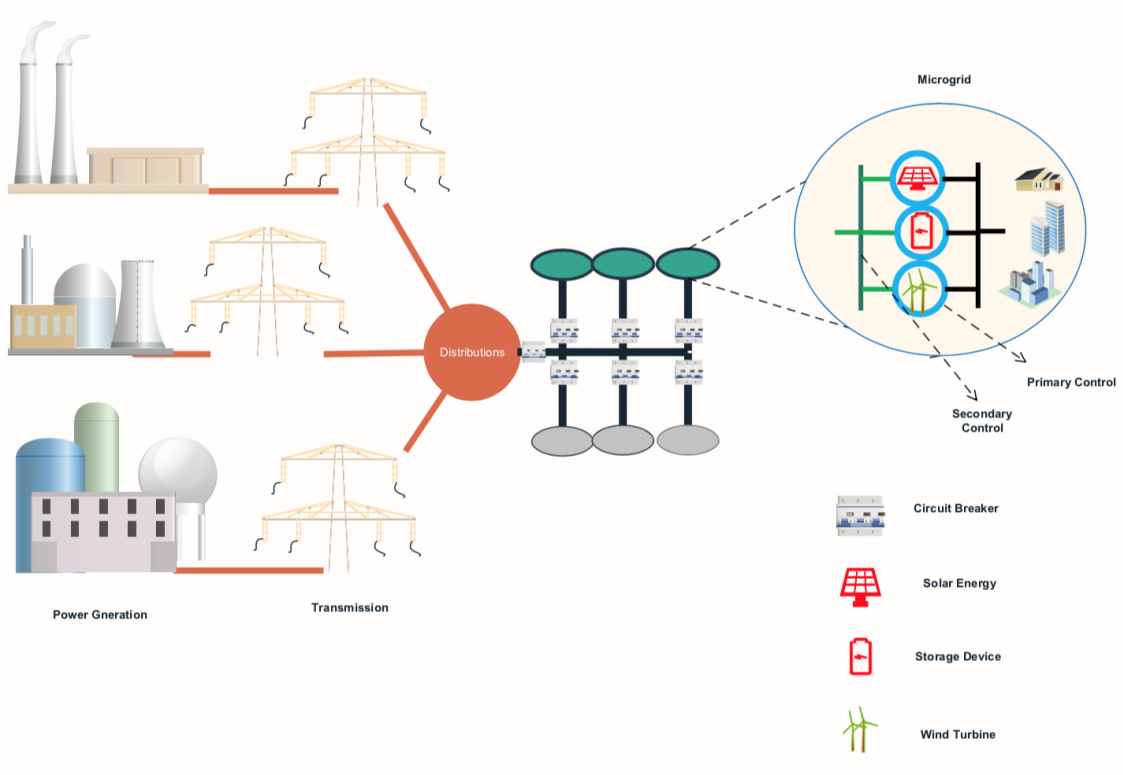

Figure 1.2: (b) Concept of new power generation systems

There are three main advantages associated with microgrids, which can be classified as: technical, economical, and environmental. From a technical perspective, distributed generation systems can support the energy of remote places and provide very high efficiency while lacking the fixed source vulnerability of large-scale networks, which is a factor in the failure of power systems [9], and [8]. From the economic point of view and according to market research studies, distributed generation minimizes line losses and interruption costs for consumers while reducing fuel cost [10]. The environmental advantages of microgrid systems are investigated in [11] and include reducing the emissions of pollutants and greenhouse gases, smaller physical footprint, and easier integration of clean energy sources.

The general configuration of a DC microgrid is shown in Fig. 1.2). Indeed, DC microgrids have several advantages over their AC counterparts such as improving the energy efficiency and the performance of power controllers and energy management schemes for regulating power flow [12, 13], and [14]. In addition, some devices such as wind turbines, electric vehicles, and electronic appliances are more easily integrated into DC than AC networks since these devices are already either DC in nature or have a different natural frequency than the primary grid. DC microgrid systems are very durable and efficient in handling voltage sags and frequency variations in the primary grid as compared with AC systems, since DC microgrids do not need frequency synchronization.

In microgrids, energy sources may be controlled by a power management system to optimize the power flow within the network. The objective of power management depends on the mode of operation such as grid connected or island modes. The main goals of the power management in grid connected mode is to stabilize the system and reduce the electricity price in the main grid. In island mode, the main objective is to optimize the microgrid operation by minimizing the cost of local generation [15], and [16].

Increasing the efficiency of power and the maximum utilization of renewable energy is

fundamental in modern power systems. Energy storage can thus be an excellent technology for this purpose [17], and [18]. When microgrids are connected to the main grid with renewable resources, the energy storage guarantees none of the energy generated is lost. For instance, if a renewable energy system such as wind is integrated to a DC microgrid without energy storage devices, the surplus power produced will be wasted if the load is not high enough. Only through the assistance of a dynamic energy storage system can utilities or system owners ensure they can store that energy for future use. Thus, microgrids with energy storage are cost effective solutions to lower overall energy costs and improve the grid's efficiency.

1.1 Energy Storage Systems

Studying energy storage systems from a power management perspective becomes significantly important for several reasons. Some of these main aspects are sizing of the energy storage, choice of the type of energy storage (e.g. lithium ion, flywheels, etc.) and optimal charging/discharging strategies.

One of the earliest types of energy storages is hydro pumps, where the power is stored in the form of water in a reservoir, whereas batteries store electrical energy in their chemistry. Moreover, energy storage is a significant microgrid component which helps the main grid in several ways such as ancillary services including load following, operational reserve, renewable integration and relieving congestion and constraints. Indeed, energy storage units must have the capability to respond sufficiently rapidly to transient power changes in grid-connected mode and to keep themselves fully charged. There are also many other applications that can utilize energy storage devices in microgrids, including consumers energy management (minimize cost) and integration of renewable energy sources.

The control of such energy storage is crucial and implementing a three-level hierarchical

control system can be used for optimum performance. For microgrids and energy storage device systems, hierarchical control can consists of three levels beginning with "primary" (for imitating physical behaviors to ensure system stability), "secondary" (for synchronizing control loops to smoothly connect or disconnect the microgrid from the distributed generation system), and "tertiary" (for controlling the power flow between the microgrid and the main grid) control levels. In this study, we focus on the tertiary control level, which relates to the control of power/energy of the microgrid resources [19].

In particular, tertiary control can be achieved solving an optimal power flow (OPF) problem: a type of optimization process with the goal of minimizing an objective function (e.g. power generation cost, losses, etc.), subject to network and physical constraints [20], and [21]. However, there are significant challenges in solving OPF problems due to its nonlinearity, non-convexity, and large scales [22]. Several numerical solution techniques are available for solving this nonlinear optimization problem. Although these techniques have been found to have capability and reliability limitations [23, 24, 25, 26, 27], and [28]. In the past decade, convex and conic relaxations have been proposed to overcome these limitations in particular for AC microgrids [29, 30], and [31].

Recently, semidefinite programming (SDP) techniques have been employed to solve the OPF problem, as described [32]. This approach is advantageous compared to the other techniques as it is convex, and easily available solvers exist for problems of moderate/large size. In some cases, the solution is globally optimal [33, 34]. The work of [35] has shown proof of concept using convex programming techniques, although the work only covers a few simple, limited systems [36].

1.2 Thesis Outline

Following the introduction in Chapter 1, Chapter 2 introduces the OPF problem. We begin by discussing the formulation and defining the general structure of an OPF problem, objective functions, state and control variables, and constraints. Thereafter, we present the difficulty of the OPF problem and the techniques to address it that are of common interest in towards solving a global optimization problem. In Chapter 3, we formulate the OPF without energy storage. In Chapter 4, we include energy storage into the OPF formulation. In Chapter 5, we test the apply the semidefinite (SDP) relaxation technique on standard test networks for the problem using a strategy based on a convex semi-definite program for the OPF problem with energy storage. Then we conclude the thesis and explore a future work in Chapter 6.

2 | AC Optimal Power Flow Problem

AC Power flow (PF) refers to the power network solution that contains complex voltages, active and reactive power, and complex currents at every bus in the specific power system [37]. In the AC PF problem, the relations between voltage/current and active/reactive power is nonlinear. Hence, obtaining a feasible set of solutions can be challenging due to this nonlinearity.

Moreover, the Optimal Power Flow (OPF) problem is an optimization problem with the main goal of minimizing the total cost of generation while at the same time meeting the power flow relationships at every bus. Hence, this problem is nonlinear and non-convex which complicates its solution. Improvement and redesign of power networks has increased the network complexity. For example, the onset of independent power and the development and production renewable generation in smart grids further extended the scope of OPF. Several contributions have been made to reformulate and improve the OPF formulation to be more efficient to handle the non-convexity problem under various hypotheses [38].

OPF problems play an essential role in power network operations and design. OPF can minimize power generation cost and losses, subject to network and physical constraints [20], and [21]. This optimization is indispensable in power network operations lasting minutes, hours, or even up to one day. The formulation of the OPF provides the optimal electrical response of the power transmission system to a specific set of power injections

and loads.

2.1 Formulation of the Optimal Power Flow Problem

As mentioned previously, the Optimal Power Flow (OPF) problem involves minimizing the total cost of generation while ensuring that the power flow equations are met at every bus. In addition, generation, voltage, and other constraints can be imposed.

In this chapter, a detailed overview of the OPF problem will be presented. This formulation will be used and expanded in the next subsections to describe algorithms that will be used for solving the OPF problem.

2.1.1 General Structure

The standard optimal power flow problem can be formulated as follows [38, 39], and [40]:

$$\min_{x,u} \quad \sum_{n=1}^{m} f_n(x,u) \tag{2.1}$$

$$\textbf{subj. to} \tag{2.2}$$

$$g(x,u) = 0 \tag{2.3}$$

$$h(x,u)^{-} \leq h(x,u) \leq h(x,u)^{+} \tag{2.4}$$

Where, $f_n(x,u)$ are cost functions, x is a vector of state variables, and u a vector of control variables, which are usually the independent variables in an OPF. The equality constraints (2.3) typically include the power flow equations at every bus. The inequality constraints (2.4) physical bounds on the state and control variables.

2.1.2 Objective Function

The most common use of the OPF objective function is to reduce the total cost of the generated power, occasionally taking an account active transmission losses in the whole or part of the power network as well. For the convergence, the generation cost functions are frequently approximated by either linear or quadratic functions [41]. In some situations, the cost is a function of both the generation active and reactive power in the network. Other types of costs which can be included in the objective function include power transfer ability, investment cost, voltage profile, load shedding, environment impact, etc [38].

2.1.3 Variables

Analysis of the OPF equations reveals two types of variables: state variables and control variables, also known as dependent and decision variables, respectively. In general, the vector states x in the OPF problems describes the electrical state of the network. These can be represented as voltage phase angles, voltage magnitudes, active power output of the slack bus only, and reactive power of all generations at each bus, including the power loads and line flows. These state variables can be represented as continuous in nature. On the other hand, the control variables u in the OPF problems normally contain a subset of the state variables and also variables describing control appliance adjustments, such as the active power at the generator buses tap changes in transformer, position of the phase shifting taps, and the status of the switched capacitors and reactors (switchable VAR sources). These control variables can be represented as continuous or discrete. The selections of the state variables x are imposed by the structure of PF equations utilized, whereas control variables vary among OPF formulations depending on the nature of the particular problem [42], and [43].

2.1.4 Constraints

Constraints are normally considered an integral part of a specific optimization problem playing a crucial role in its categorization, for example, convex vs non-convex. In the OPF problem, the network variables have to be within allowable bounds or else damage the electrical power network devices or cause a malfunction. Typically, the constraints are classified as equality and inequality constraints [42], and [43].

In OPF problems, equality constraints are normally represented by the power flow system equations [44]. Inequality constraints identify upper and lower bounds on the control and state variables of the devices of the electrical power network and also the bounds required to ensure network security and stability [40]. The inequality constraints on the state variables and controls can be partitioned as follows:

- **State Variables Bounds on**
  - Voltage Magnitude.
  - Voltage Angle.
  - Power Line.
- **Control Variables Bounds on**
  - Active Power Generation.
  - Reactive Power Generation.
  - Volt Ampere Reactive Power.
  - Voltage Generation.
  - Transformer Tap Position.

Moreover, the inequality constraints can also define forbidden areas of branch flow limits, interface limits, active/reactive power reserve limits, spinning reserve requirements,

transient security, transient stability, transient contingencies, environment constraints, rotor angle stability, etc. [45].

2.1.5 Standard Optimal Power Flow (OPF) Problem

In this subsection, we present two mathematical models of the power system networks and show their equivalence. Let the set of buses be $\mathcal{N}$:=$\{1, 2, 3, .., n\}$, the set of transmission lines $\mathcal{E} \subseteq \{\mathcal{N} \times \mathcal{N}\}$ of edges. Then $n \sim j$ denotes a line between the buses n and j.

2.1.5.1 Bus Injection Model (BIM):

The general bus injection model (BIM) is defined by the following power flow equations that represent Kirchhoff's laws at each bus

$$S_n = \sum_{j:n\sim j} V_n(V_n^H - V_j^H)y_{nj}^H, \forall n \in \mathcal{N} \tag{2.5}$$

the superscript H denotes hermitian transpose. Let the set the solutions of the power flow V for each S to be:

$$\mathcal{V} := \{V \in \mathbb{C}^{(n+1)} |\ V \text{ satisfies } (2.5)\} \tag{2.6}$$

The buses in the power networks can be divided into three classes: slack, generation, and load buses. The next quantities are generally identified at each bus: voltage phase angles δ, voltage magnitudes $|V|$, active power output of the slack bus only P_s, and reactive power of all generations Q_n. Usually the voltage magnitudes and the angles are described by one complex variable V rather than real and imaginary variables. Let us now consider the general power network modeled by the subset of buses $\mathcal{N}$:=$\{1, 2, 3, .., n\}$, the set of transmission lines $\mathcal{E} \subseteq \{\mathcal{N} \times \mathcal{N}\}$ of edges, and the set of generation buses $\mathcal{G} \subset \mathcal{N}$.

- $P_n^d + iQ_n^d$: Complex power of the load connected to bus $n, \forall n \in \mathcal{N}$.

- $P_n^g + iQ_n^g$: Complex power output of the generator connected to bus $n, \forall n \in \mathcal{N}$
- V_n: Complex voltage at bus $n, \forall n \in \mathcal{N}$.
- y_{nj}: Admittance of the transmission line $(n, j) \in \mathcal{E}$, $y_{nj} = g_{nj} + ib_{nj}$.

Define V, P^g, Q^g, P^d and Q^d as the vectors formed stacking, in lexicographical order the values at all the buses of the corresponding variables V_n, P_n^g, Q_n^g, P_n^d, and Q_n^d $\forall n \in \mathcal{N}$, respectively. Assume $f_n(\cdot)$ is a convex function representing the cost associated with bus $n \in \mathcal{N}$. The objective is to minimize the total cost of the system. This problem can then be formulated as follows:

$$\min_{P_n^g, V_n} \quad f = \sum_{n \in \mathcal{N}} f_n(P_n^g) \tag{2.7}$$

$$\textbf{subj. to} \tag{2.8}$$

$$|V_n^-| \leq V_n \leq |V_n^+|, \quad \forall n \in \mathcal{N} \tag{2.9}$$

$$P_n^{g-} \leq P_n^g \leq P_n^{g+}, \quad \forall n \in \mathcal{N} \tag{2.10}$$

$$Q_n^- \leq Q_n \leq Q_n^+, \quad \forall n \in \mathcal{N} \tag{2.11}$$

$$P_n^g + Q_n^g = P_n^d + Q_n^d + V_n \sum_{j:n\sim j}^{n \in \mathcal{N}} \left\{ V_n - V_j^H \right\} y_{nj}, \forall n \in \mathcal{N} \tag{2.12}$$

$$|V_n - V_j| \leq \Delta V_{nj}^+, \forall (n, j) \in \mathcal{E} \tag{2.13}$$

In this formulation P_n^g and Q_n^g are controllable variables, and P_n^d and Q_n^d are given external disturbances. The solution will give values of P_n^g and Q_n^g, at every bus, that minimize the cost and satisfy the physical and operational constraints of the network. In the remainder of this work we specialize to DC power systems where $Q_n^g = Q_n^d = 0$ and the constraints are P_n^-, P_n^+, P_n^d, V_n^-.

2.2 Hardness of Optimal Power Flow (OPF) problem

There are three main challenges that must be faced in the numerical solution of OPF problems: 1) the presence of constraints, 2) the nonlinear nature of constraints and 3) switching elements and scale of the system.

2.2.1 Active Constraints:

Given a feasible point, the inequality requirements satisfied at this point with strict imbalances are called latent or inactive, while those limitations satisfied with equality are alluded to as binding or active constraints. Finding the dynamic inequality limitations has a combinatorial viewpoint, and it is a troublesome piece of tackling the OPF problem. Indirect approaches exist for solving OPF without utilizing a middle optimization approach to obtain the active sets at an optimal solution [46].

2.2.2 Non-Convexity:

Despite the fact that some OPF problems can be formulated with linear objective function, the problem is nonlinear due to the power flow equations being nonlinear as shown in (2.12). Subsequently, the non-convex feasible sets may even be unconnected. Therefore, the **Karush–Kuhn–Tucker** (KKT) conditions are not usually adequate for a global optimum. Specifically, for AC power systems, the OPF problem is naturally non-convex and allows for many local optimal solutions. Correspondingly, existing solution approaches utilized extensively in practice depend on repeated optimization approaches, which can only return local optimal solutions with the achievement of a global optimal solution. In summary, the non-convexity of the OPF problem broadly prohibits obtaining a solution in polynomial time, which makes OPF NP-hard to achieve [12].

2.2.3 Switching Behavior:

Tackling dual and integer variables that arise when representing node levels switch controls in practical power systems introduces a significant level of difficulty due to the fact the OPF becomes an integer programming problem. In addition increasing power network size increases the computational complexity significantly [34].

2.3 Techniques to solve Optimal Power Flow (OPF) problem

2.3.1 Optimization Techniques

Many different approaches have been proposed to solve OPF problem, including linear programming (LP), quadratic programming (QP), nonlinear programming (NLP), and interior point methods (IPM). However, these approaches have not been widely used in industry according to [47]. As is to be expected there is no single approach that can be used for all OPF problems, even though a few approaches might be more successful than others in certain OPF problems. Some of the figures of merit used to compare algorithms utilized in OPF problems, reported in [48], and [49] include accuracy, computational speed, robustness, flexibility, scalability, solution quality, and rate of convergence. It is very challenging for a single algorithm to hold all these characteristics. However, solution quality, robustness, rate of convergence, reliability, and scalability are of primary importance in selecting an OPF optimization approach [49]. In this subsection, some of these approaches are described in detail.

2.3.2 Traditional Optimization Methods

Examples of traditional optimization algorithms for solving the OPF problem include: Newton-like method, sequential linear programming (SLP), non-linear programming (NLP), simplex method (SM), lambda-iterative methods (LIM), successive quadratic programming (SQP), and gradient-based methods [47], and [50]. The simplex approach is appropriate for LP-based OPF problems and can be directly applied to the DC-OPF formulation [27], and [51]. SLP is an extension of LP described by [52] that allows for optimizing problems with nonlinear characteristics by a sequence of linear approximations. In certain cases, a NLP formulation can be reduced to an LP by utilizing linear approximations of the objective function and constraints around an initial estimate of the optimal solution [23, 53], and [54]. SQP is a solution method for NLP problems, and similar to SLP, it solves the original problem by solving a sequence of QP problems, of which solutions converge to a global optimal solution of the original problem [55]. In most SQP implementations for an OPF problem, conventional power flow equations are linearized at each iteration, which can increment the computational effectiveness at the cost of an increase in the number iterations. Many studies have investigated the implementation of SQP for solving OPF problems [56, 57], and [58]. The following technique centers on directly solving the NLP problem rather than solving a sequence of LP or QP approximation problems.

2.3.2.1 Gradient Techniques (GT):

This approche was among the first efforts in the late 1960s to find solution to OPF problems. Gradient techniques can be split into three essential paths of exploration: reduced gradient techniques (RG), conjugate gradient techniques (CG), and generalized reduced gradient techniques (GRG). Gradient technique generally utilize the first-order derivative vector $\nabla f(x_k)$ of the objective function at the first iterate x_k to decide an enhancing heading. Gradient technique are not difficult to ensure convergence of correct functions. However,

gradient technique is slow, i.e., requests additional repetition contrasted to higher-order technique. Furthermore, since it does not use the second-order derivative, it may converge to a local optimal point. Global optimality must be confirmed for nonconvex problems, which eliminate most OPF formulations [20], and [12]. The RG technique has been used to find a solution to the OPF problem by [59]. The CG technique is essentially an enhancement and a change of the RG technique and is a standout amongst the most understood iterative techniques for taking care of NLP problems with sparse systems of linear equations. Rather than utilizing the negative reduced gradient as the heading of descent, the CG technique selects the descent trends such that it is conjugate to the past search trends by including the present negative gradient vector to a scaled, linear combination of past search trends. There are a few focal points of applying CG technique for resolving an OPF problem, especially the enhancement and change of the characteristics over the RG technique [60]. The GRG technique is an augmentation and an expansion of the RG technique, which empowers coordinate treatment of inequality and nonlinear constraints. Instead of utilizing penalty functions, the GRG technique modifies the iterations by inserting slack variables with all inequality limitations and all constraints are linearized about the present working point. In this manner, the first problem is moved into a progression of subproblems with linear constraints that can be determined by RG or CG techniques [61]. Be that as it may, since linearization presents a hitch in the constraints, an extra advance is required to adjust the variables toward the finish of every repetition with emphasis to recuperate feasibility. In the OPF, this feasibility recuperation is performed by explaining a regular power flow [62].

2.3.2.2 Newton's Techniques (NT):

Newton's technique (NT) is essentially a second-order method for unconstrained optimization based on Taylor series expansion. The descent trend at a point x_k is set to $d_k = -H(x_k)^1 \nabla f(x_k)$, where $H(x_k)$ indicates the Hessian matrix of f at point x_k. Then the tech-

nique figures out a step size $\alpha_k > 0$ in trend d_k satisfying confirmed step-size choosing principles such as inexact line seeking with fall back. However, the technique does not ensure to converge to a local optimum solution as the Hessian matrix H may not be positive semidefinite in an adequately large neighborhood of the lower or minimum point. The NT requires the application of Lagrangian function when utilized to OPF problems. Inequality constraints produced from the power system physical edges must either be neglected or handled as equality, relying on whether they are bounded at either the optimal solution or not. However, recognizing active inequality constraints is the main challenge for Newton-based solutions for OPF problem, as mentioned in *Section* 2.2. In one study, [63] presented a Newton-based OPF technique and another investigation by [64] discussed a more effective approach applying the Lagrangian function. Thus researchers have made momentous contributions to improve performance of power active inequality constraints [65].

2.3.2.3 Interior Point Methods (IPM):

The challenge of implementing inequality constraints was a motivating factor for employing interior point methods (IPMs) to solve OPF problems. IPMs are a family of projective scaling approaches for solving linear and nonlinear optimization problems. IPMs are used to define and follow a central path through the feasible district to the set of optimal solutions. The main point of feasibility enforcement is achieved either by utilizing partition terms in the augmented objective function or by manipulating the required KKT conditions [66]. When utilized to solve OPF problems, IPMs have been developed over the past decades. The most well-known techniques are the primal-dual interior-point method (PDIPM) [67], Mehrotra's predictor-corrector techniques [68], Gondzio's multiple-centrality corrections [69], and trust district techniques [70]. Among various IPMs, PDIPMs are probably the most popular deterministic approaches studied in OPF research. Granville [71] was the first to employ PDIPMs to the OPF problem, extending

first PDIPMs for LP and QP to the NLP case of reactive power dispatch. The main features of Newton's technique contain no requirement to define the active constraint set or have an initial feasible solution. Several types of research on IPMs have focused on enhancing PDIPMs by taking advantage of the framework of power flow constraints. For instance, [72] suggested a changed PDIPM which utilizes a feature function to promote the convergence properties for OPF. A simplified OPF formulation utilizing rectangular coordinates and present mismatches described by [73] leads to a facilitation of Hessian matrix and can reduce computational effort.

2.3.3 Convex Relaxation for Optimal Power Flow (OPF) problem

The traditional techniques for solving the non-linear and non-convex OPF problems have been described in *subsection* 2.3.2. Some of these techniques rely on KKT conditions, which can only assure a local optimal solution because of the non-convexity of the OPF problem. Furthermore, the characteristics of the nonlinearity and the non-convexity of the problem make the OPF problem NP-hard to solve. Taking into account that the OPF formulation has been specified in *subsection* 2.1.5, the non-convexity of the problem dictates power flow equation constraints (2.12). For each connection line $(n, j) \in \mathcal{E}$, let $y_{nj} = a_{nj} + ib_{nj}$ indicate its admittance, and $Y \in \mathbb{C}^{\mathcal{N}\times\mathcal{N}}$ indicate the admittance matrix of the power network, i.e.,

$$Y_{nj} := \begin{cases} -y_{nj}^{ref}, & if \;\; n \neq j \;\; and \;\; (n, j) \in \mathcal{E} \\ \sum_{l\in\mathcal{N}(n)} y_{nl}, & if \quad n = j \\ 0, & \text{Otherwise} \end{cases} \tag{2.14}$$

where $\mathcal{N}(n)$ is known as set of buses at certain bus. Let I_n indicates the current of bus n, and $I := [I_1 I_2 ... I_N]^T$ indicate the current vector of all buses, which can be written as YV,

and $S_n = P_n + iQ_n$ indicate the net power injection of bus n, i.e.,

$$S_n = P_n + iQ_n = (P_{G_n} - P_{D_n}) + i(Q_{G_n} - Q_{D_n}) \tag{2.15}$$

The state of each bus can be written as:

- **Current balance**

$$I_n = \sum_{j \in \mathcal{N}(n)} y_{nj}(V_N - V_j), \forall n \in \mathcal{N} \tag{2.16}$$

- **Power balance**:

$$S_n = V_n I_n^*, \forall n \in \mathcal{N} \tag{2.17}$$

Define e_1, e_2,..., e_N as the standard basis vectors in $\mathcal{R}^N$ such that $(e_n)_j = 0$ if $n \neq j$, $(e_n)_j = 1$ if $n = j$. Therefore,

$$S_n = P_n + iQ_n = (P_{G_n} - P_{D_n}) + i(Q_{G_n} - Q_{D_n}) = V_n I_n^* = (e_n^* V)(e_n^* Y V)^* = e_n^* V V^* Y^* e_n = \boldsymbol{Tr}(V V^* Y^* e_n e_n^*) \tag{2.18}$$

1. **Semidefinite Relaxation (SDP)**:

   As mentioned earlier, the nonlinearity and non-convexity of the OPF problem make it NP-hard. Thus, let the non-linear term VV^* in equality constraint (2.3) be changed by a new matrix variable $M \in H^{N \times N}$ to define this constraint as a linear term and to be convex, where $H^{N \times N}$ indicates the set of $N \times N$ of Hermitian matrices. At the same time, in order to make sure that the map from V to M is invertible, M must be constrained to be both positive semidefinite and rank-one. The feasible set of main OPF problem in *subsection* 2.1.5 can be equivalently formulated as follows (for clarity, the transmission line constraints have been emitted but will be considered

later):

$$P_n^{g^-} \leq P_n^g \leq P_n^{g^+}, \quad \forall n \in \mathcal{N} \tag{2.19}$$

$$Q_n^{g^-} \leq Q_n^g \leq Q_n^{g^+}, \quad \forall n \in \mathcal{N} \tag{2.20}$$

$$(V_n^-)^2 \leq M_{nn} \leq (V_n^+)^2, \quad \forall n \in \mathcal{N} \tag{2.21}$$

$$TR(MY^* e_n e_n^*) = (P_{G_n} - P_{D_n}) + i(Q_{G_n} - Q_{D_n}), \quad \forall n \in \mathcal{N} \tag{2.22}$$

$$M = M^* \tag{2.23}$$

$$\boldsymbol{Rank}(M) = 1 \tag{2.24}$$

However, the rank constraint (2.24) makes OPF formulation non-convex. Eliminating this rank constraint from the optimization problem creates the SDP relaxation, which is defined as a convex problem unless the objective function is a non-convex function. SDP relaxation can be solved effectively and easily in polynomial time. However, the main challenge is qualifying the solution for the relaxation to match the optimal solution of the original non-convex problem. In some scenarios the relaxation is strict. In [34], it has been proved that the dual of the original OPF problem is the same as the dual of the SDP relaxation; under certain circumstances, robust duality holds between the SDP relaxation and the dual of the original OPF problem with quadratic generation cost. Generally, the dual optimal value is only a lower limit on the optimal objective value of the OPF problem and the lower limit may not be strict in the presence of a nonzero duality gap. Moreover, it has been shown that the global optimal solution to the OPF problem can be restored from the optimal solution to the convex dual problem whenever the duality gap between the dual and the original OPF problem is 0. In this scenario, the SDP relaxation is strict, the OPF problem can be obtained either by utilizing SDP or dual relaxation. Reference, [34] proposed solving the dual of the OPF problem instead of the primal SDP relaxation as the number of variables in the primal SDP relaxation increases quadratically with

the number of nodes in the network, while the number of variables in the dual problem grows linearly with the number of nodes. This uniqueness is especially valuable when utilizing primal and dual interior-point algorithms for solving the primal SDP and dual relaxations, respectively [34]. In their approach, a necessary and adequate situation is provided to assure the existence of zero duality gap for the OPF problem, which is created for the standard IEEE benchmark systems with 14, 30, 57, 118, and 300 buses including various randomly generated networks. Taking into consideration the hardness of demonstrating this situation, another approach has been studied to assure the existence of zero duality gap for the IEEE model. In this situation, a small perturbation is inserted into the admittance matrix that holds well in practice. In addition, the duality gap is predicted to be zero for a large bus of power systems due to the passivity of transmission lines and transformers [34]. More recent approaches have been proposed with other sources of non-convexity in OPF, such as variable transformer ratios, variable shunt elements and contingency constraints [74]. In addition to quadratic cost functions, the previous work on OPF with arbitrary convex cost functions have been developed by [28]. In [28], they found that because of the physics of the power network, every OPF problem can be effectively solved in polynomial time after applying the following approximations:

- Write power balance equations as inequalities, and
- Place all equalities and the unknown parameters of the system.

2. **Second-Order Cone Relaxation (SOCP)**:

   SOCP relaxation a linear function is minimized over the intersection of an affine set and the product of second-Order cones. SOCP relaxation is nonlinear convex problem that involve linear and quadratic program as special cases. However, SOCP relaxations have a much lower computational complexity than the SDP relaxations. The main challenge of solving the OPF problem comes from the nonlinear equality

constraints in (2.12). To avoid this problem, one can approximate the feasible set of OPF problem with a convex set via change of variables: $\forall n \in \mathcal{N}$, define

$$U_{nj} = V_n V_j \ , n \sim j \tag{2.25}$$

For each line $n \sim j$ where $n < j$, let $\boldsymbol{H}^{2\times 2}$ as follow

$$M_{nj} = \begin{bmatrix} v_n & U_{nj} \\ U_{jn} & v_j \end{bmatrix} \in \boldsymbol{H}^{2\times 2} \tag{2.26}$$

By introducing the new (slack) variable U_{nj}, the feasible set of the OPF problem can be expressed as

$$P_n^g - P_n^d = \sum_{j:n\sim j}^{n\in\mathcal{N}} \left(v_n - U_{nj}\right) y_{nj}, \forall n \in \mathcal{N} \tag{2.27}$$

$$P_n^{g-} \leq P_n^g \leq P_n^{g+}, \ \ \forall \ n \in \mathcal{N} \tag{2.28}$$

$$v_n^- \leq v_n(\kappa) \leq v_n^+, \ \ \forall \ n \in \mathcal{N} \tag{2.29}$$

$$M_{nj} = \begin{bmatrix} v_n & U_{nj} \\ U_{jn} & v_j \end{bmatrix} \geq 0, \forall n \sim j \tag{2.30}$$

$$\boldsymbol{Rank(M_{nj})} = 1 \quad \forall n \sim j \tag{2.31}$$

In this transformation, the rank constraint is a non-convex set. To recover convexity the feasible set can be relaxed by removing the rank constraint (2.31). If in addition the cost function to be minimized is convex the problem becomes an SOCP, because the set of positive semidefinite matrices defines a conic constraint. This will be referred as the SOCP relaxation of the OPF [12].

While contrasting the SDP relaxation and SOCP relaxation for OPF problem, we notice that the SDP relaxations have a matrix variable M with $\frac{N\times(N+1)}{2}$ unknown entries; as a consequence the number of decision variables in the SDP is N^2. Subsequently,

it can be challenging to obtain effectively while increasing N. On the other hand, the SOCP relaxations are more memory efficient than SDP relaxations because it enforces constraints only on the sub-matrices of M. Furthermore, the SOCP relaxations have a lower computational complexity.

The SOCP relaxation is said to be exact when the solution for the original OPF problem satisfies the rank one constraint. When the relaxation is exact the solution of the SOCP is also a global optimal solution of the original OPF problem [22].

A number of researchers have proposed different SOCP relaxations that guarantee exactness that exploit particular characteristics of the power system [20]. For instance, in [75] it is shown that their SOCP relaxation can be exact for radial networks.

Other approaches include [20] and [75]. They suggested some adjustments to the OPF formulation with imposing slightly different voltage magnitude lower and upper bounds in (2.9). This makes it possible to prove that the SOCP relaxation for the adjusted OPF problem is exact. There is no guarantee that the adjustment OPF problem will have a feasible set that is close to that of the original OPF problem. Hence, the solution obtained with this approach may not be close to the global solution of the original OPF problem. On the other hand, [20] and [75] reported favorable numerical results for IEEE test networks demonstrating that the SOCP relaxations may work well in practice but with no guarantees.

3 | Optimal Power Flow without Energy Storage

3.1 Notation

In this section, the notation of the DC system is presented which will be used for the rest of the paper. The DC model contains buses and lines connecting all buses with each others. These lines can be linked in tree, mesh, and radial topologies, Fig. (3.1) shows.

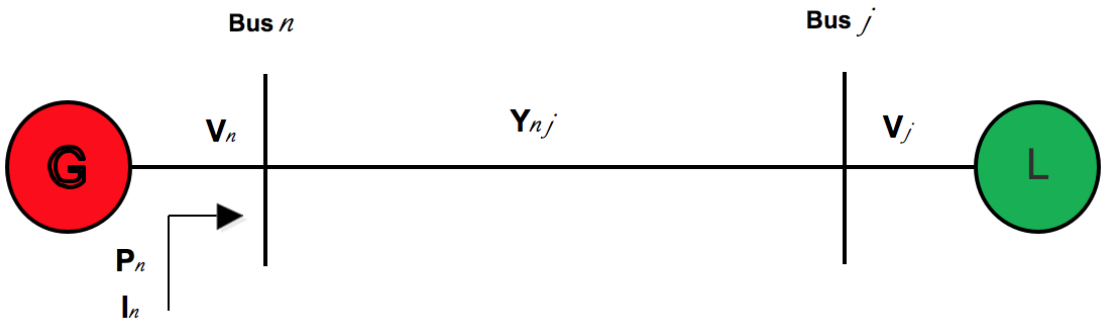

Figure 3.1: Summary of notation.

The graph $\mathcal{G}$:=$\{\mathcal{N}, \mathcal{E}\}$ contains a set $\mathcal{N}$ of nodes and a set $\mathcal{E}$ of edges. Each line connects an ordered pair (n, j) of buses. If two buses n and j are connected by a tie line directly, we denote $(n, j) \in \mathcal{E}$ by $n \sim j$. For each bus $n \in \mathcal{N}$, V_n represents its voltage, I_n represents the current injection, and P_n represents the power injection. At each line, let y_{nj} represents the admittance, and I_{nj} represents the current flow between buses $n \sim j$ from n to j, also $Z_{nj} := \frac{1}{y_{nj}}$ it is impedance. For each bus $n \in \mathcal{E}$, let $P_n^g(t)$ denotes the generation at time t and $P_n^d(t)$ denote its constant load demand. Notice that all the above parameters are real numbers since we are working in DC network.

3.2 Mathematical Model and Problem Formulation

3.2.1 Analysis of Optimal Power Flow without Energy Storage

In this section, we present a derivation of optimal power flow problem. This formulation does not include energy storage elements and a fully connected 3 bus system as shown in Fig.(3.2). The Power flows in network are controlled by the following physical rules:

$$I_{nj} = (V_n - V_j) y_{nj} \ , \forall \{n, j\} \in \mathcal{E} \qquad \textbf{(Ohm's Law)}$$

$$I_n = \sum_{j:n\sim j} (I_{nj}) \ , \forall \{n, j\} \in \mathcal{N} \qquad \textbf{(Current balance)}$$

$$P_n = V_n I_n \ , \forall \{n, j\} \in \mathcal{N} \qquad \textbf{(Power Balance)}$$

Therefore, the power flow at bus n satisfies:

$$P_n^g - P_n^d = V_n \sum_{j:n\sim j} (V_n - V_j) y_{nj} \ , \quad \forall \{n, j\} \in \mathcal{N} \tag{3.1}$$

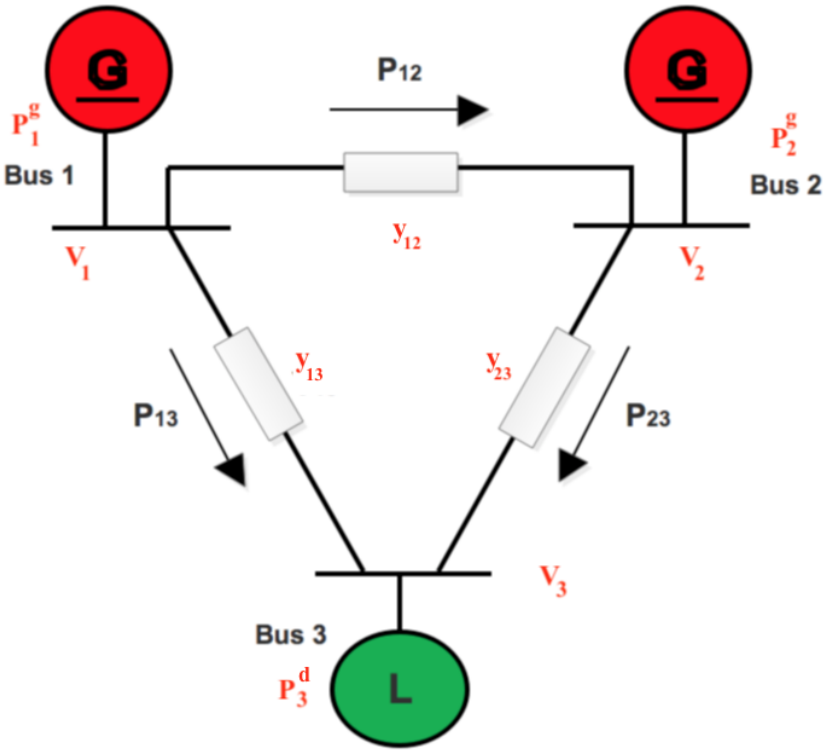

Figure 3.2: 3-bus of Power system.

Then, the optimal power flow problem for this particular example is:

$$\min_{P_n^g, V_n} \quad \sum_{n \in \mathcal{N}} f_n(P_n^g) \tag{3.2}$$

subj. to (3.3)

$$P_n^g - P_n^d = V_n \sum_{j:n\sim j}^{3} (V_n - V_j) y_{nj} \quad n = 1, \ldots, 3 \tag{3.4}$$

$$P_n^{g-} \leq P_n^g \leq P_n^{g+}, \quad n = 1, \ldots, 3 \tag{3.5}$$

$$V_n^- \leq V_n \leq V_n^+, \quad n = 1, \ldots, 3 \tag{3.6}$$

The cost (3.2) is a function of generation in each node The equality constraint (3.4) is non-linear in V_n and nonconvex. It can be replaced by a linear constraint on VV^T with a new matrix variable $U{:=}VV^T$ and $V_n = [V_1, V_2, V_3]^T$. However, to make the map from V to U invertible, U must be constrained to be positive semidefinite (SDP) with rank equal to one. Relaxing the rank constraint (removing it) leads to a second-order cone programming

(SOCP) problem. The resulting OPF is:

$$\min_{P_n^g, V_n, M_{nj}} \quad \sum_{n \in \mathcal{N}} f_n(P_n^g), \quad \forall n \in \mathcal{N} \tag{3.7}$$

$$\textbf{subj. to} \tag{3.8}$$

$$P_n^g - P_n^d = \sum_{j:n\sim j}^{n\in\mathcal{N}} \Big(v_n - U_{nj}\Big) Y_{nj}, \forall n \in \mathcal{N} \tag{3.9}$$

$$P_n^{g-} \leq P_n^g \leq P_n^{g+}, \quad \forall n \in \mathcal{N} \tag{3.10}$$

$$v_n^- \leq v_n \leq v_n^+, \quad \forall n \in \mathcal{N} \tag{3.11}$$

$$M_{nj} = \begin{bmatrix} v_n & U_{nj} \\ U_{jn} & v_j \end{bmatrix} \geq 0 \quad \forall n \sim j \tag{3.12}$$

As mentioned above, if the solution fo the SOCP problem satisfies the rank one constraint it is also a global solution to the original non-convex OPF. Eliminating the rank one constraint results in a convex problem by enlarging the feasible set; however, the new feasible set is larger than that of the original OPF problem. That is why checking the rank condition a posteriory is necessary.

3.3 Demonstration and Evaluation of Proposed Optimal Power Flow (OPF) Method

3.3.1 Introduction

This section demonstrates the OPF algorithm by testing a six-bus system described in [76]. We will begin by implementing the OPF algorithm using both a Matlab nonlinear programming solver and using the special solver CVX which is a Matlab software for solving a complex convex optimization problems; files required for this case study can be found in [77] and [78]. The computer specification for running this algorithm is a Lenovo Intel Core i5 DDR3 SDRAM (2410M Cache, 2.30 GHz) with 8GB memory.

3.3.2 System Description

The Six-bus system is illustrated in Fig.5.3 [76]. The unit data for this system are given by Table. (3.1)

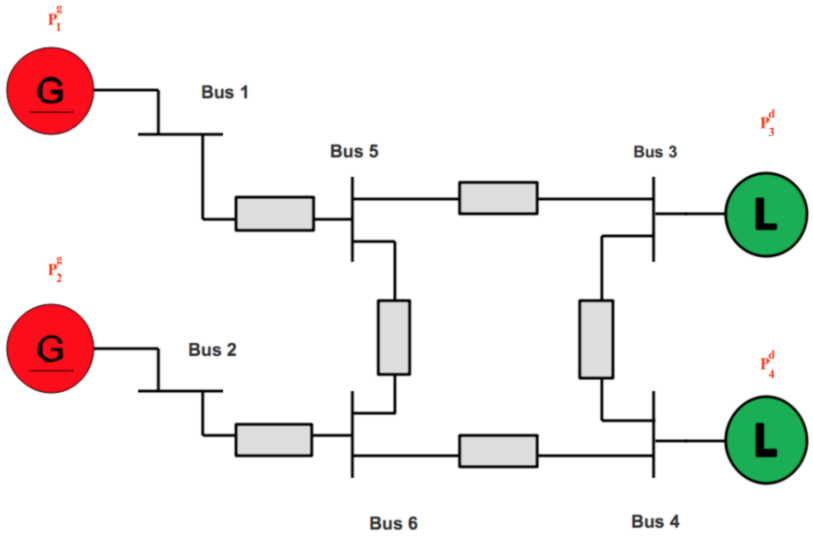

Figure 3.3: 6-bus of Power System.

BUS	Cost Function	V_n^-	V_n^+	P_n^{g-}	P_n^{g+}	P_n^d
1	5	350	450	0	10,000	0
2	7	350	450	0	10,000	0
3	0	350	450	0	10,000	10,000
4	0	350	450	0	10,000	6,000
5	0	350	450	0	10,000	0
6	0	350	450	0	10,000	0

Table 3.1: DC Microgrid Parameters.

The conductances between each bus are shown in table.3.2.

From BUS	To BUS	Conductances
1	5	0.5
5	3	0.02
3	4	0.02
4	6	0.02
6	2	0.5
6	5	0.02

Table 3.2: Conductances Between Lines

In this test system, there are two power loads (P_n^d) and two generators dispatched. The power loads (P_3^d and P_4^d) at bus 3 and 4 are set to be 10 KWh and 6 KWh, respectively. The cost function values are also set to $P_1^g = 5$ \$/MWh and $P_2^g = 7$ \$/MWh. At each bus, the power variables are bounded to between 0 and 10 KWh and the voltage constraints are set between 350 V and 450 V.

3.3.3 Solution to Nonlinear OPF

Based on the system described in the previous subsection, the general OPF problem is as follows:

$$\min_X f = [5P_1^g + 7P_2^g] \tag{3.13}$$

$$X^T := \begin{bmatrix} P_1^g & P_2^g & V_1 & V_2 & V_3 & V_4 & V_5 & V_6 \end{bmatrix}$$

subj. to (3.14)

$$P_1 = P_1^g - P_1^d = V_1(V_1 - V_5)y_{15} \tag{3.15}$$

$$P_2 = P_2^g - P_2^d = V_2(V_2 - V_6)y_{26} \tag{3.16}$$

$$P_3 = P_3^g - P_3^d = V_3(V_3 - V_4)y_{34} + V_3(V_3 - V_5)y_{35} \tag{3.17}$$

$$P_4 = P_4^g - P_4^d = V_4(V_4 - V_3)y_{43} + V_4(V_4 - V_6)y_{46} \tag{3.18}$$

$$P_5 = P_5^g - P_5^d = V_5(V_5 - V_1)y_{51} + V_5(V_5 - V_3)y_{53} + V_5(V_5 - V_6)y_{56} \tag{3.19}$$

$$P_6 = P_6^g - P_6^d = V_6(V_6 - V_2)y_{62} + V_6(V_6 - V_4)y_{64} + V_6(V_6 - V_5)y_{65} \tag{3.20}$$

$$[P_n^g,\ P_n^d,\ V_n] = \begin{cases} 0 \le P_1^g \le 10K \\ 0 \le P_2^g \le 10K \\ 350 \le V_{[1,..,6]} \le 450 \\ V_{1_{ref}}^{ref} = 380 \\ P_3^d = 10K \\ P_4^d = 6K \end{cases}$$

Where $V_{[1,..,6]}$ represents the voltages at each bus.

3.3.3.1 Solution Report and Analysis

In this example, the optimal cost is $9,5615\$/hour$.The final result is shown by

Bus	P_n^g	V_n
1	10,000	380
2	6,5164	375.48
3	0	366.36
4	0	366.42
5	0	366.84
6	0	366.80

Table 3.3: Matlab-Nonlinear programming solver Result

The solver takes 10 iterations to reach the minimum cost of the system with 1.123837 second of total CPU time.

3.3.4 Solution to Convex Relaxation of OPF

Using the convex relaxation technique, we can obtain the following problem:

$$\min_X f = [5P_1^g + 7P_2^g] \tag{3.21}$$

$$X^T := \begin{bmatrix} P_1^g & P_2^g & v_1 & v_2 & v_3 & v_4 & v_5 & v_6 & U_{nj} \end{bmatrix}, \quad \forall n \sim j$$

subj. to (3.22)

$$P_1 = P_1^g - P_1^d = (v_1 - U_{15})y_{15} \tag{3.23}$$

$$P_2 = P_2^g - P_2^d = (v_2 - U_{26})y_{26} \tag{3.24}$$

$$P_3 = P_3^g - P_3^d = (v_3 - U_{34})y_{34} + (v_3 - U_{35})y_{35} \tag{3.25}$$

$$P_4 = P_4^g - P_4^d = (v_4 - U_{43})y_{43} + (v_4 - U_{46})y_{46} \tag{3.26}$$

$$P_5 = P_5^g - P_5^d = (v_5 - U_{53})y_{53} + (v_5 - U_{51})y_{51} + (v_5 - U_{56})y_{56} \tag{3.27}$$

$$P_6 = P_6^g - P_6^d = (v_6 - U_{64})y_{64} + (v_6 - U_5)y_{65} + (v_6 - U_{62})y_{62} \tag{3.28}$$

$$[P_n^g,\ P_n^d,\ V_n] = \begin{cases} 0 \le P_1^g \le 10K \\ 0 \le P_2^g \le 10K \\ 350 \le V_{[1,..,6]} \le 450 \\ V_{1_{ref}}^{ref} = 380 \\ P_3^d = 10K \\ P_4^d = 6K \end{cases}$$

Where $v_{[1,..,6]}$ represents the voltage square at each bus.

Therefore, the M_{nj} in OPF can be formulated as follows: In the relaxation step, the rank constraint $\boldsymbol{Rank}(M_{nj})$ is eliminated, but a positive semidefinite constraint $M_{nj} \succeq 0$ needs to be kept. We refer to this relaxation as SDP hereafter.

$$R := \begin{bmatrix} M_{nj} & & \\ & \ddots & \\ & & M_{nj} \end{bmatrix} \succeq 0 \quad \forall i \sim j \tag{3.29}$$

3.3.4.1 Solution Report and Analysis

In this example, the optimal cost is 95244.5\$/*hour*.The final result is shown by

No.	P_n^g	v_n	$V_n=\sqrt{v_n}$	$M_{nj}=\sqrt{V_{nj}^2}$
1	10,000	14440	380	13940
2	6,5164	14980	374.48	13773
3	0	13422	366.42	13424
4	0	13426	366.42	13439
5	0	13457	366.84	13440
6	0	13454	366.80	13456

Table 3.4: CVX Result

By (2.30), (2.31), and (3.29) the matrix of R can be obtained as follows:

$$R := \begin{bmatrix} \begin{bmatrix} v_1 & U_{15} \\ U_{51} & v_5 \end{bmatrix} & & & & & & \\ & \begin{bmatrix} v_2 & U_{26} \\ U_{62} & v_6 \end{bmatrix} & & & & & \\ & & \begin{bmatrix} v_3 & U_{34} \\ U_{43} & v_4 \end{bmatrix} & & & & \\ & & & \begin{bmatrix} v_4 & U_{46} \\ U_{64} & v_6 \end{bmatrix} & & & \\ & & & & \begin{bmatrix} v_5 & U_{53} \\ U_{35} & v_3 \end{bmatrix} & & \\ & & & & & \begin{bmatrix} v_6 & U_{65} \\ U_{56} & v_5 \end{bmatrix} \end{bmatrix} \geq 0 \tag{3.30}$$

The solver takes 22 iterations to reach the minimum cost of the system with 2.51 second

of total CPU time, 0.11 second per iteration.

3.3.5 Result Summary

This chapter presented the OPF solution of six-bus system via the linear power system model. The results showed that the CVX solver is more effective and accurate than non-linear programming for large-scale system. Moreover, the minimum solution satisfied constraints. Nevertheless, the final cost using the Matlab nonlinear programming solver was $9,5615\$/hour$, which was very close to the final cost using the CVX solver.

4 | Optimal Power Flow with Energy Storage

4.1 Notation

In this chapter, we first review the notation. A Graph $\mathcal{G}:=\{\mathcal{N}, \mathcal{E}\}$ contains a set $\mathcal{N}$ of nodes and a set $\mathcal{E}$ of edges. Each line connects an ordered pair (n, j) of buses. If two buses n and j are connected by a tie line directly, we denote $(n, j) \in \mathcal{E}$ by $n \sim j$. For each bus $n \in \mathcal{N}$, $V_n(\kappa)$ represents its voltage. At each line let y_{nj} represents the conductance between bus $n \sim j$ from n to j. For each bus $n \in \mathcal{N}$, let $P_n^g(\kappa)$ denotes the generation, $P_n^d(\kappa)$ its load demand at time κ and $b_n(\kappa)$ the value of the energy storage at time κ. The energy storage elements a modeled by the difference equation (4.1). It can therefore be considered as the following collection of discrete linear time-varying models (one for each $\tau = \{1, ..., (M)\}$), whose state at time κ (going backward in time) is $\kappa \in \tau$. It also can be assumed that T_s represents the time step of the time series. Moreover, $r_n(\kappa)$ represents the value of the power at time (κ) where it charges when $r_n(\kappa)$ has a negative value; $r_n^- < 0$. Otherwise it discharges when $r_n(\kappa)$ has a positive value; $r_n^+ \geq 0$. In addition, B_n^- and B_n^+ represent the minimum and maximum value of the energy storage, respectively.

4.2 The Optimal Power Flow with Energy Storage

An OPF problem optimizes both variables V and P over the feasible solutions of the bus injection model in (3.4). Additionally, all voltage magnitudes must satisfy (3.11) where the lower and upper bounds are represented by V_n^- and V_n^+. The lower bound of voltage magnitude is assumed to be greater than zero to avoid triviality in the system. The power injection is also bounded as shown in (3.10), similar to the case of the voltage magnitudes, where P_n^- and P_n^+ are given bounds on the injections at bus n. We now formulate an OPF with energy storage and time-varying generation costs and demands. As mentioned previously, $b_n(\kappa)$ represents the value of the energy storage at time κ at bus n. The amount of the energy storage is modeled to follow the first order difference equation.

$$b_n(\kappa + 1) = b_n(\kappa) + \alpha_n r_n(\kappa), \quad \forall n \in \mathcal{N}, \quad \kappa \in \tau \tag{4.1}$$

where α_n denotes the time interval $[\kappa, \kappa+1]$. Assuming the initial energy stored is $b_n(0) \geq 0$ at each bus $n \in \mathcal{N}$

$$0 \leq B_n^- \leq b_n(\kappa) \leq B_n^+, \quad \forall n \in \mathcal{N}, \quad \kappa \in \tau \tag{4.2}$$

where B_n^- and B_n^+ represent the minimum and maximum value of the energy storage at bus n, respectively. Moreover, the charge rate of the battery are bounded by:

$$r_n^- \leq r_n(\kappa) \leq r_n^+, \quad \forall n \in \mathcal{N}, \quad \kappa \in \tau \tag{4.3}$$

where κ=1, ..., $(\tau + 1)$. The power flow constraint at each bus $n \in N$ and time $\kappa \in \tau$ are thus:

$$P_n^g(\kappa) - P_n^d(\kappa) - r_n(\kappa) = \sum_{j:n\sim j}^{n\in\mathcal{N}} \Big(v_n(\kappa) - U_{nj}(\kappa)\Big) Y_{nj}, \forall n \in \mathcal{N}, \ \kappa \in \tau \tag{4.4}$$

where $P_n^g(\kappa)$ represents the generation at bus n at time κ and $P_n^d(\kappa)$ represents its load.

Thus, OPF problem with energy storage in DC microgrid can be formulated as follows:

$$\min_{P_n^g(\kappa),V_n(\kappa),b_n(\kappa),r_n(\kappa)} \quad \sum_{n\in\mathcal{N}}\left\{\sum_{\kappa=1}^{M} f_n(P_n^g(\kappa)) + h_n^{\kappa}(b_n(\tau))\right\}, \ \ \forall n \in \mathcal{N}, \quad \kappa \in \tau \tag{4.5}$$

subj. to (4.6)

$$V_n^- \leq V_n(\kappa) \leq V_n^+, \ \ \forall n \in \mathcal{N}, \quad \kappa \in \tau \tag{4.7}$$

$$P_n^{g-} \leq P_n^g(\kappa) \leq P_n^{g+}, \ \ \forall n \in \mathcal{N}, \quad \kappa \in \tau \tag{4.8}$$

$$r_n^- \leq r_n(\kappa) \leq r_n^+, \quad \forall n \in \mathcal{N}, \quad \kappa \in \tau \tag{4.9}$$

$$b_n^- \leq b_n(\kappa) \leq b_n^+, \quad \forall n \in \mathcal{N}, \quad \kappa \in \tau \tag{4.10}$$

$$b_n(\kappa+1) = b_n(\kappa) + \alpha_n r_n(\kappa), \quad \forall n \in \mathcal{N}, \quad \kappa \in \tau \tag{4.11}$$

$$P_n^g(\kappa) - P_n^d(\kappa) - r_n(\kappa) = \sum_{j:n\sim j}^{n\in\mathcal{N}} \left(V_n^2(\kappa) - V_n(\kappa)V_j(\kappa)\right) y_{nj}, \forall n \in \mathcal{N}, \ \kappa \in \tau \tag{4.12}$$

- **The Initial Condition (I.C) of b_n at $\kappa = 0$**

$$b_n(0) = \mu_c, \quad \forall n \in \mathcal{N} \tag{4.13}$$

- **The Voltage Reference at bus n_{ref}**

$$V_{n_{ref}}^{ref}(\kappa) = V_0 \tag{4.14}$$

Now, we present the convex formulation of the OPF problem with energy storage:

$$\min_{P_n^g(\kappa),v_n(\kappa),b_n(\kappa),r_n(\kappa),U_n(\kappa)} \quad \sum_{n\in\mathcal{N}}\left\{\sum_{\kappa=1}^{M} f_n(P_n^g(\kappa)) + h_n^{\kappa}(b_n(\tau))\right\}, \ \forall n \in \mathcal{N}, \quad \kappa \in \tau \tag{4.15}$$

subj. to (4.16)

$$v_n^- \le v_n(\kappa) \le v_n^+, \ \forall n \in \mathcal{N}, \quad \kappa \in \tau \tag{4.17}$$

$$P_n^{g-} \le P_n^g(\kappa) \le P_n^{g+}, \ \forall n \in \mathcal{N}, \quad \kappa \in \tau \tag{4.18}$$

$$r_n^- \le r_n(\kappa) \le r_n^+, \quad \forall n \in \mathcal{N}, \quad \kappa \in \tau \tag{4.19}$$

$$B_n^- \le b_n(\kappa) \le B_n^+, \quad \forall n \in \mathcal{N}, \quad \kappa \in \tau \tag{4.20}$$

$$b_n(\kappa+1) = b_n(\kappa) + \alpha_n r_n(\kappa), \quad \forall n \in \mathcal{N}, \quad \kappa \in \tau \tag{4.21}$$

$$P_n^g(\kappa) - P_n^d(\kappa) - r_n(\kappa) = \sum_{j:n\sim j}^{n\in\mathcal{N}} \Big(v_n(\kappa) - U_{nj}(\kappa)\Big) Y_{nj}, \forall n \in \mathcal{N}, \ \kappa \in \tau \tag{4.22}$$

$$M_{nj} = \begin{bmatrix} v_n & U_{nj} \\ U_{jn} & v_j \end{bmatrix} \succeq 0, \quad \forall n \sim j \tag{4.23}$$

$$\boldsymbol{Rank}(M_{nj}) = 1 \tag{4.24}$$

where v_n:=V_n^2 and U_{nj}:=$V_n V_j$ $\forall n \sim j$.

Since (4.24) is a non-convex constraint, it must be relaxed to arrive at the convex formulation. Also, f_n has to be a convex function.

- **The Initial Condition (I.C) of b_n at $\kappa = 0$**

$$b_n(0) = \mu_c, \quad \forall n \in \mathcal{N} \tag{4.25}$$

- **The Voltage Reference at bus n_{ref}**

$$V_{n_{ref}}^{ref}(\kappa) = V_0 \tag{4.26}$$

Equation (4.1) is often written in term of the State-of-Charge, $SOC_n(\kappa) := \frac{b_n(\kappa)}{E_{tot}}$, where E_{tot} is the total energy. Hence it is equivalent to

$$SOC_n(\kappa + 1) = SOC_n(\kappa) + \alpha_n r_n(\kappa), \quad \forall n \in \mathcal{N}, \quad \kappa \in \tau \tag{4.27}$$

where, α_n is $\frac{T_s}{E_{tot}}$. With respect to SOC inequalities (4.20) became

$$SOC_n^- \leq SOC_n(\kappa) \leq SOC_n^+, \quad \forall n \in \mathcal{N}, \quad \kappa \in \tau \tag{4.28}$$

where

- $f_n(P_n^g)$ is a convex cost function, which represents generation.
- $h_n^\kappa(b_n(\tau))$ represents the terminal cost.

4.2.1 Optimal Power Flow with Line Constraints

It is also possible to limit the current going through any line $n \sim j$. Let I_{nj} be a threshold of the current flow through $n \sim j$, then the line constraint can be formulated as:

$$(v_n - U_{nj} - U_{jn} + v_j) y_{nj}^2 \leq I_{nj}^2 \tag{4.29}$$

which in terms of original voltage variables is:

$$(V_n - V_j)^2 y_{nj}^2 \leq I_{nj}^2 \tag{4.30}$$

Adding (4.29) to the constraints of the OPF problem leads to :

$$\min_{P_n^g(\kappa),v_n(\kappa),SOC_n(\kappa),r_n(\kappa),U_n(\kappa)} \quad \sum_{\kappa=1}^{M}\left\{\sum_{n\in\mathcal{N}} f_n(P_n^g(\kappa)) + h_n^{\kappa}(b_n(\tau))\right\}, \quad \forall n\in\mathcal{N}, \quad \kappa\in\tau \tag{4.31}$$

subj. to (4.32)

$$v_n^- \le v_n(\kappa) \le v_n^+, \quad \forall n\in\mathcal{N}, \quad \kappa\in\tau \tag{4.33}$$

$$P_n^{g-} \le P_n^g(\kappa) \le P_n^{g+}, \quad \forall n\in\mathcal{N}, \quad \kappa\in\tau \tag{4.34}$$

$$r_n^- \le r_n(\kappa) \le r_n^+, \quad \forall n\in\mathcal{N}, \quad \kappa\in\tau \tag{4.35}$$

$$B_n^- \le SOC_n(\kappa) \le B_n^+, \quad \forall n\in\mathcal{N}, \quad \kappa\in\tau \tag{4.36}$$

$$SOC_n(\kappa+1) = SOC_n(\kappa) + \alpha_n r_n(\kappa), \quad \forall n\in\mathcal{N}, \quad \kappa\in\tau \tag{4.37}$$

$$P_n^g(\kappa) - P_n^d(\kappa) - r_n(\kappa) = \sum_{j:n\sim j}^{n\in\mathcal{N}} \Big(v_n(\kappa) - U_{nj}(\kappa)\Big)Y_{nj}, \forall n\in\mathcal{N}, \kappa\in\tau \tag{4.38}$$

$$\Big(v_n(\kappa) - U_{nj}(\kappa)\Big)Y_{nj} \le P_{nj} \tag{4.39}$$

$$\Big(v_j(\kappa) - U_{jn}(\kappa)\Big)Y_{jn} \le P_{jn} \tag{4.40}$$

$$M_{nj} = \begin{bmatrix} v_n & U_{nj} \\ U_{jn} & v_j \end{bmatrix} \succeq 0, \quad \forall n\sim j \tag{4.41}$$

One way to keep some of the theoretical ensures is to force the line constraints in terms of power flows alternatively. In specific, $|I_{nj}| \le \hat{I}_{nj}$ is equivalent to $|P_{nj}| \le V_n\hat{I}_{nj}$. Assuming that V_n is near to its nominal value, then $|P_{nj}| \le V_n\hat{I}_{nj}$ can be proximated by $|P_{nj}| \le \hat{P}_{nj}$ for some $\hat{P}_{nj} \in \mathcal{R}$. Hence, the final formulation of the line constraints can be written as (4.39) and (4.41).

(For detailed proofs, see $\boldsymbol{Theorem-7}$ in [20]).

4.2.2 Modeling the Energy Storage

Assuming that bus n can have at most one battery for energy storage, we denote SOC_n the charge of the battery at bus n. For simplicity, batteries were modeled as discrete-time integrators:

$$SOC_n(\kappa + 1) = SOC_n(\kappa) + \alpha_n r_n(\kappa), \quad SOC_n(0) \text{ given} \tag{4.42}$$

where α_n [h/KW] is the event sampling and $r_n(\kappa)$ the rate of charge. In the rest of this section, we will show how to express the dynamic equations imposed by the battery as algebraic linear equations suitable for inclusion in a non dynamic optimization problem.

Consider a causal linear, time-invariant, discrete-time system with the state-space equations

$$\begin{aligned} x(\kappa + 1) &= Ax(\kappa) + Bu(\kappa), \quad x(0) = x_o \\ y(\kappa) &= Cx(\kappa) + Du(\kappa) \end{aligned} \tag{4.43}$$

where x is the state vector and u the input vector.

The general expression for the solution of the state-space equations is

$$x(\kappa) = A^{\kappa} x_o + \sum_{m=0}^{\kappa-1} A^{(\tau-1)-m} Bu(m), \quad \kappa \geq 0 \tag{4.44}$$

In the context of OPF problems, τ is the index of the planning epoch. Suppose that the problem involves (M) epochs, starting at $M = 1$. Then (4.44) can be written in matrix form

as:

$$x(M) - A^M x_o = \begin{bmatrix} A^{M-1}B & \cdots & AB & B \end{bmatrix} \begin{bmatrix} u(0) \\ u(1) \\ \vdots \\ u(M-1) \end{bmatrix}$$

Collecting all the states at each epoch in a vector, we obtain the following linear algebraic equation:

$$\begin{bmatrix} x(1) \\ x(2) \\ \vdots \\ \vdots \\ x(M) \end{bmatrix} - \begin{bmatrix} A \\ A^2 \\ \vdots \\ \vdots \\ A^M \end{bmatrix} x_o = \begin{bmatrix} B & 0 & \cdots & \cdots & 0 \\ AB & B & \ddots & & 0 \\ & \ddots & \ddots & \ddots & \vdots \\ A^{M-2}B & & \ddots & B & 0 \\ A^{M-1}B & A^{M-2}B & \cdots & AB & B \end{bmatrix} \begin{bmatrix} u(0) \\ u(1) \\ \vdots \\ \vdots \\ u(M-1) \end{bmatrix}$$

For the particular model of the battery in (4.42) the above equations reduce to

$$\begin{bmatrix} SOC_n(1) \\ SOC_n(2) \\ \vdots \\ \vdots \\ SOC_n(M) \end{bmatrix} - \begin{bmatrix} 1 \\ 1 \\ \vdots \\ \vdots \\ 1 \end{bmatrix} SOC_n(0) = \begin{bmatrix} \alpha_n & 0 & \cdots & \cdots & 0 \\ \vdots & \ddots & \ddots & & 0 \\ \vdots & & \ddots & \ddots & \vdots \\ \vdots & & & \ddots & 0 \\ \alpha_n & \cdots & \cdots & \cdots & \alpha_n \end{bmatrix} \begin{bmatrix} r_n(0) \\ r_n(1) \\ \vdots \\ \vdots \\ r_n(M-1) \end{bmatrix} \tag{4.45}$$

5 | Demonstration and Evaluation of Proposed OPF Method with Energy Storage

5.1 Introduction

This section demonstrates the DC-OPF problem with energy storage by testing a six-bus system [76]. This problem is a nonconvex optimization problem whose objective function has discontinuous first order derivatives that we solved through a special CVX solver and ran on a Lenovo Intel Core i5 DDR3 SDRAM (2410M Cache, 2.30 GHz) with 8GB memory.

5.2 CASE STUDIES

5.2.1 Test Case of DC Microgrid System

The first test case considers DC microgrid system, with two separate power sources — the DC network and a battery device — directly connected to the microgrid through a bus. The battery device is added to the grid to provide sufficient power to the loads, in case of the local power is not enough or if a generator fails.

5.2.2 Scenario-I, Parameters and Results

The microgrid, is a system of six buses shown in Fig. 5.1. The network consists of two power generators at buses 1 and 2, two loads at buses 3 and 4, four link buses (i.e., without generation nor load) and eight transmission lines. An energy storage unit has added to bus 6. Since the full life of a battery device is directly related to the number of charging and discharging cycles, there is a cost associated with it a per charge cycle [79]. The parameters and the boundary conditions associated with the power generators, the SOC, and the bus reference are given in Table. 5.1 and the power loads at different operational times are given in *Appendix – I* Table. 7.1. The line constraints are given in Table. 5.2. The costs of power purchased from the generators are set to P_1^g = 5\$/MWh and P_2^g = 7\$/MWh. The voltage magnitude bounds for all buses are set between 350 V and 450 V, and the voltage magnitude at the first bus defined as a reference bus, V_1^{ref}, is 380 V.

BUS	V_n^-	V_n^+	P_n^{g-}	P_n^{g+}	$V_{n_{ref}}^{ref}$	SOC_n^-	SOC_n^+	r_n^-	r_n^+
1	-	-	0	10K	380	-	-	-	-
2	350	450	0	10K	-	-	-	-	-
3	350	450	-	-	-	-	-	-	-
4	350	450	-	-	-	-	-	-	-
5	350	450	-	-	-	-	-	-	-
6	350	450	-	-	-	0.2	0.8	-7K	7K

Table 5.1: The bound constraints.

BUS	$\Delta V_{nj}(\kappa)^-$	$\Delta V_{nj}(\kappa)^+$
3 To 4	-2K	2K
4 To 3	-2K	2K
5 To 6	-2K	2K
6 To 5	-2K	2K

Table 5.2: The power capacity constraints.

In this scenario, the transmission lines between buses 5 and 6 and between buses 3 and 4 are bounded. The storage battery is bounded by a capacity $SOC_n(\kappa)^-$ and $SOC_n(\kappa)^+$ with a

charge or discharge rate (discussed earlier) as $r_n(\kappa)^-$and $r_n(\kappa)^+$. The initial condition of the storage battery was chosen to be 0.7 KWh. A total of 20 KWh of energy was proposed as well as the sampling time of one hour, and the simulations were performed over one day. The simulation results illustrate the advantages of including an energy storage under low and high demand circumstances. During low demand, the energy is stored in the storage unit and then released when the load is high, smoothing the total power injected into the grid.

5.2.3 Demonstration of Scenario-I

The system in Fig. 5.1 includes a storage device at bus 6.

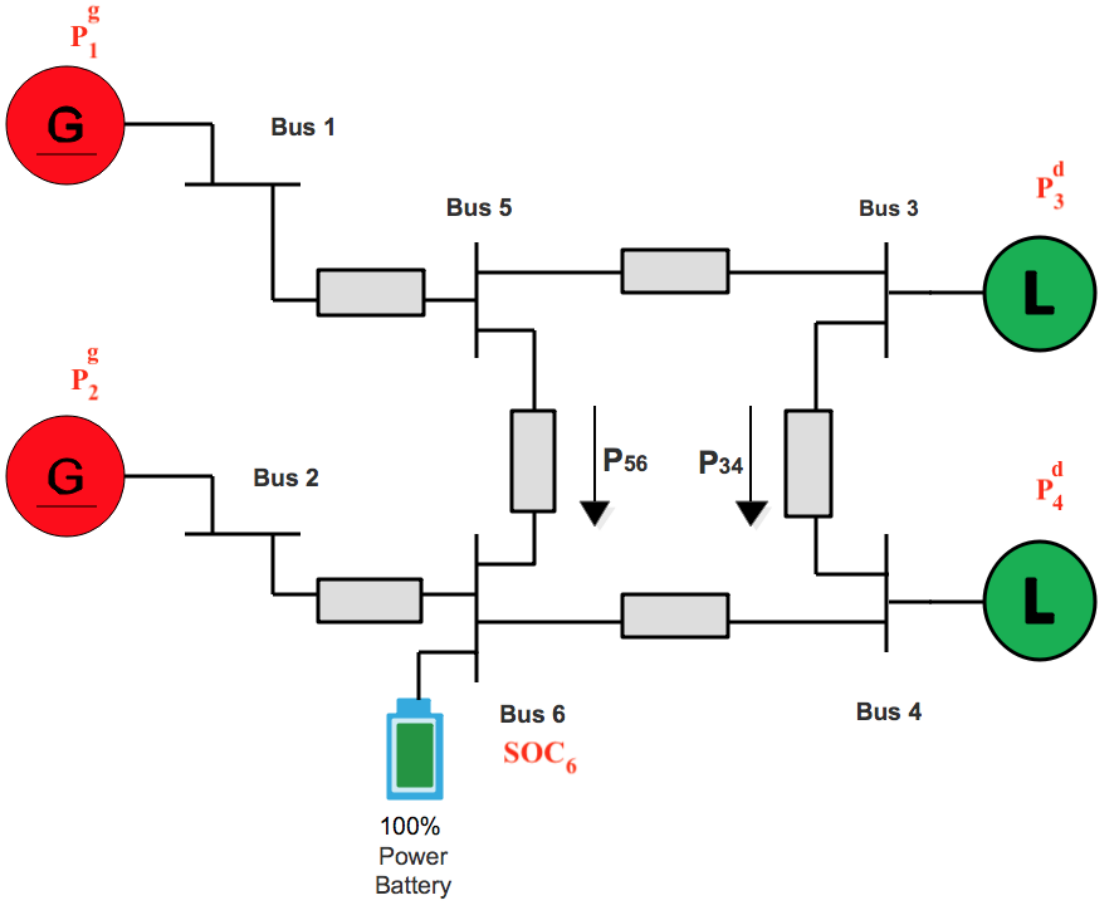

Figure 5.1: Scenario I: A power system with energy storage at bus six.

The following description as mentioning earlier: power generations are represented by P_n^g, storage power is $r_n(\kappa)$, and the event sampling is α_n. The battery is modeled by its minimum and the maximum value of the energy storage $r_n(\kappa)^-$ and $r_n(\kappa)^+$, and the battery State of Charge SOC_n, in the range 0.2 and 0.8. This represents energy in this problem.

$$\min_{P_n^g(\kappa), v_n(\kappa), SOC_n(\kappa), r_n(\kappa), U_n(\kappa)} \quad \sum_{\kappa=1}^{24} \sum_{n \in 6} f_n(5P_1^g(\kappa) + 7P_2^g(\kappa)) \tag{5.1}$$

subj. to (5.2)

$$380 \leq v_n(\kappa) \leq 450, \quad \forall n \in 6, \quad \kappa \in \tau \tag{5.3}$$

$$0 \leq P_1^g(\kappa) \leq 10K, \quad \kappa \in \tau \tag{5.4}$$

$$0 \leq P_2^g(\kappa) \leq 10K, \quad \kappa \in \tau \tag{5.5}$$

$$-7K \leq r_6(\kappa) \leq 7K, \quad \kappa \in \tau \tag{5.6}$$

$$0.2 \leq SOC_6(\kappa) \leq 0.8, \quad \kappa \in \tau \tag{5.7}$$

$$SOC_6(\kappa + 1) = SOC_6(\kappa) + \alpha_6 r_6(\kappa), \quad \kappa \in \tau \tag{5.8}$$

$$P_{[1,2]}^g(\kappa) - P_{[3,4]}^d(\kappa) - r_6(\kappa) = \sum_{j:n\sim j}^{n \in 6} \Big\{ v_n(\kappa) - U_{nj}(\kappa) \Big\} Y_{nj}, \forall n \in 6, \ \kappa \in \tau \tag{5.9}$$

$$-2K \leq \Big\{ v_n(\kappa) - U_{nj}(\kappa) \Big\} Y_{nj} \leq 2K \tag{5.10}$$

$$-2K \leq \Big\{ v_j(\kappa) - U_{jn}(\kappa) \Big\} Y_{jn} \leq 2K \tag{5.11}$$

$$\boldsymbol{R} := \begin{bmatrix} \boldsymbol{M}_{nj} & & \\ & \ddots & \\ & & \boldsymbol{M}_{jn} \end{bmatrix} \geq 0, \quad \forall n \sim j \tag{5.12}$$

- **The Initial Condition (I.C) of SOC_6 at $\kappa = 0$**

$$SOC_6(0) = 0.7 \tag{5.13}$$

- **The Voltage Reference at bus n_{ref}**

$$V_{n_{ref}}^{ref}(\kappa) = 380 \tag{5.14}$$

The problem was solved numerically using CVX. The results are summarized in Table. 5.3.

Optimal value	505927
Computation Time (s)	0.12

Table 5.3: The result of Scenario-I.

It was verified, a posteriory, that the rank one conditions on $M_{nj}, \forall\ n \sim j$ were satisfied. Hence the optimal value of the cost reported in the table is also global optimum for the original OPF. The numerical values of power injections and nodal voltages are listed in Appendix-I, Tables. 7.2 and 7.3.

5.2.4 System Load Data

The total power load of the DC microgrid for each hour is shown in Fig. 5.2. This includes the power loads at buses 3 and 4. The power load at bus 3 is constant during the operational time. However, the power load at bus 4 is unsteady with the average hourly power load of around 7.5 KWh.

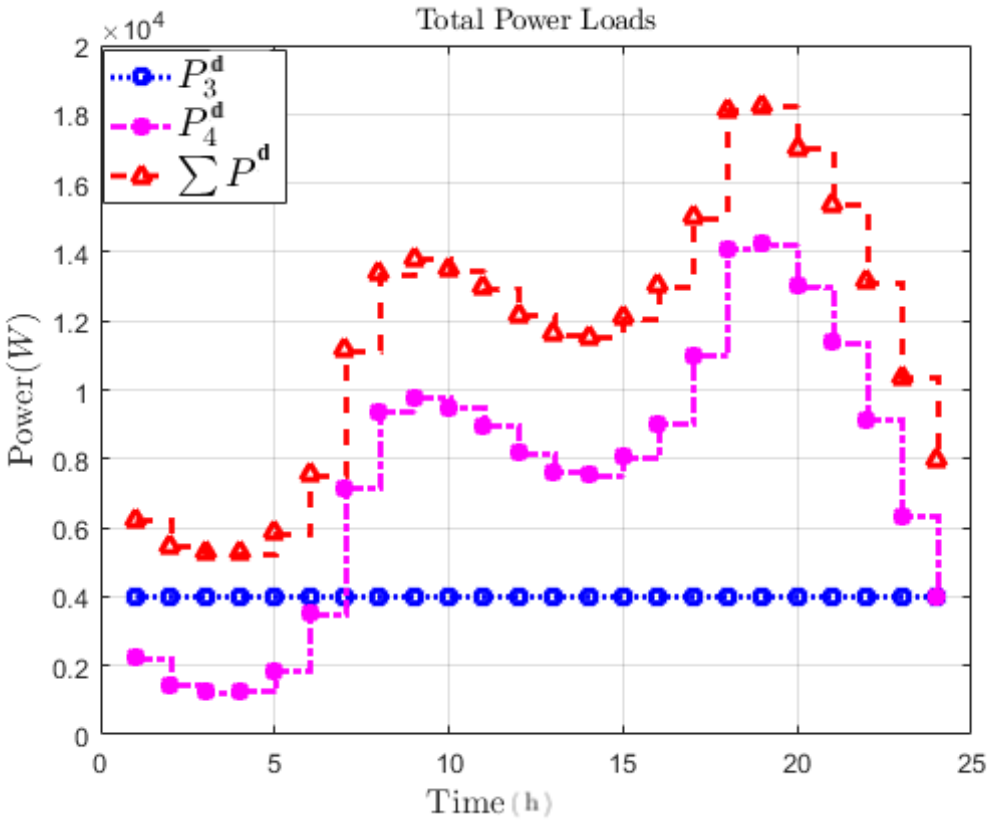

Figure 5.2: The actual power loads

5.2.5 System Generation Data

The power generator schedule for the 24 hours is given in Fig. 5.3, which illustrates that all generators during the operational time are within the bounds and satisfied the constraints.

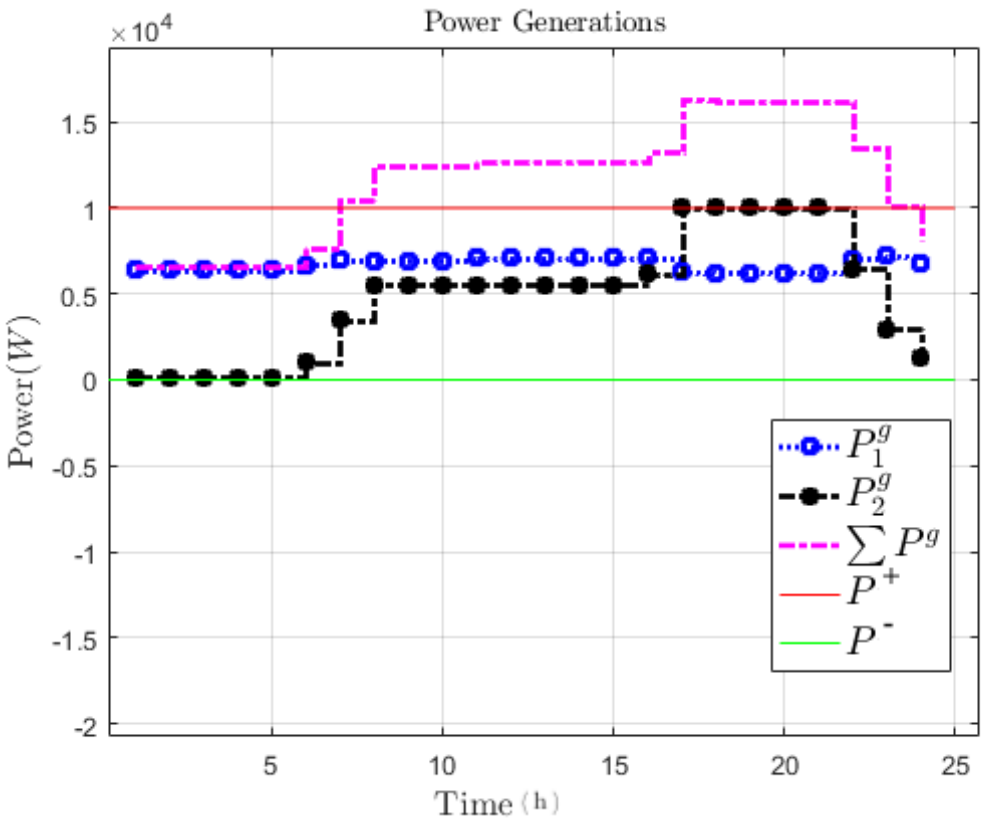

Figure 5.3: The generator schedule

In Fig. 5.4, it can been seen that the battery schedule satisfied the constraints and bounds during the operations. Moreover, battery charging and discharging happen during the production times as can be seen by noting the graphs. The energy stored in the battery is charging during 1 to 6, 11 to 16, and between 23 to 24. It is also discharging during 7 to 10 and between 17 to 22. The stored power is utilized to feed nearby loads and avoid losses and the high cost on the system if faraway the DC generations are used to feed these loads. Since the battery is not needed to hold any further power at the end of 25 hours, it

is economically beneficial to discharge all the battery energy so the net battery energy is 0. The total optimal cost for supplying the load is given in Table. 5.3.

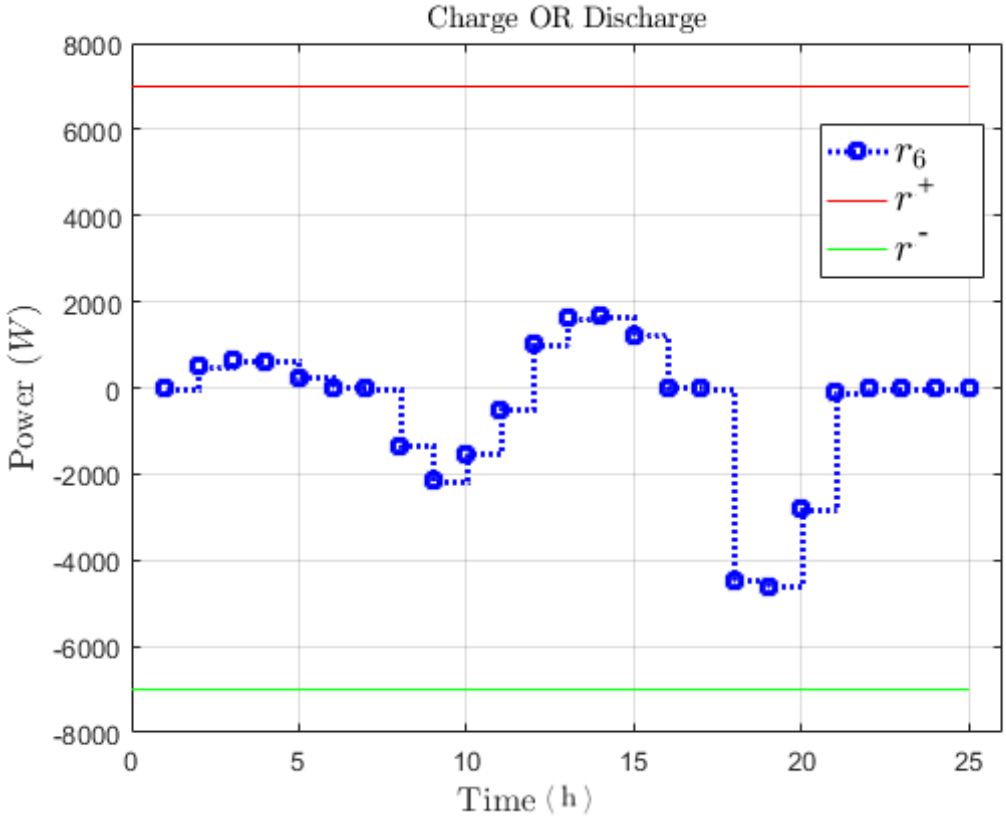

Figure 5.4: The battery schedule

A list of the standby power battery values are given in Appendix-I, Table. 7.3. These values are required at each hour to support the system by providing energy necessary for the loads.

5.2.6 State-of-Charge (SOC)

A dynamic OPF problem has been solved due to the dynamics of the state-of-charge (SOC) of the battery. As shown in Fig. 5.5, it can be seen experimentally when the battery is either charged fully $SOC = 100\%$ or discharged to $SOC = 0\%$.

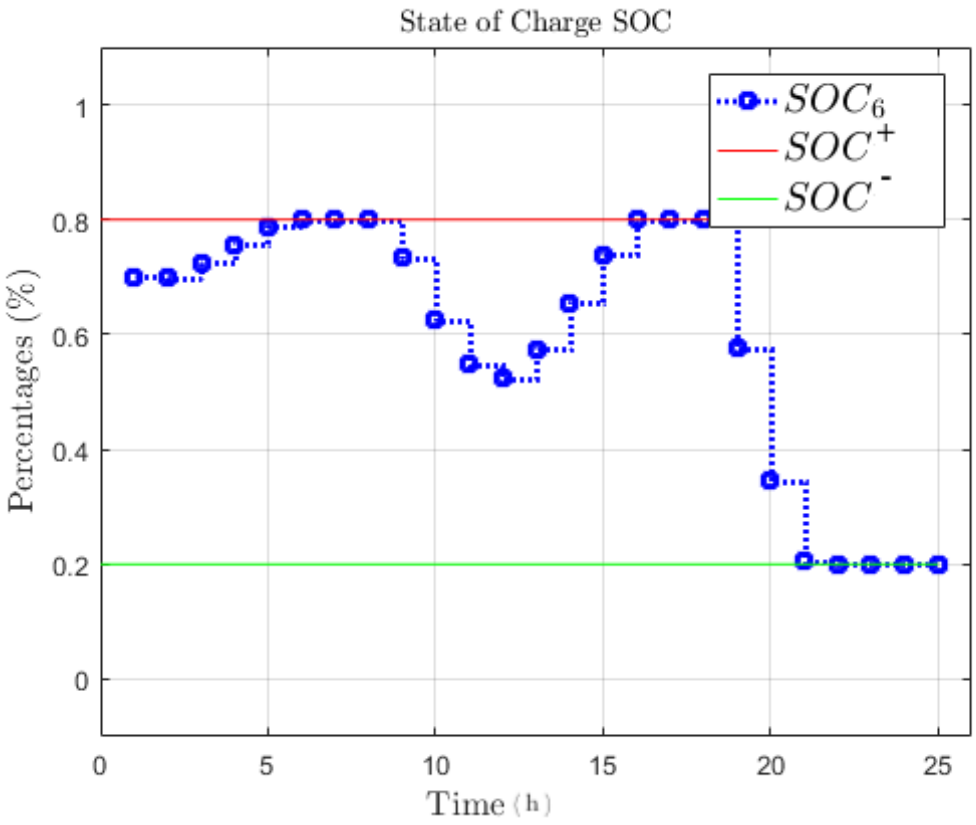

Figure 5.5: The State-of-charge schedule

5.2.7 Parameters and Results of Scenario-II

In this scenario, the OPF formulation with energy storage dynamics are applied to examine the reliability and stability of the system. The DC microgrid is, shown in Fig. 5.6. Presently the network consists of two power generators at buses 1 and 2, two loads at buses 3 and 4, and four link buses (i.e., without including generation nor load) and eight transmission lines. Furthermore, two energy storage units have been applied in the network at buses 5 and 6. The main aim of including a battery device in this system is to increase system security by acting as a standby when required. The parameters and the constraints in the system associated with the power generators, the SOC, and the bus reference are shown in Table. 5.4, and the power loads at different operational time are given in Appendix-II Table. 7.4. Moreover, the line constraints have been considered in this case as shown in Table. 5.5. The costs of power purchased to the main grid throughout the operation are also set to P_1^g = 5\$/MWh and P_2^g = 7\$/MWh. The voltage magnitude V_n bounds for all buses are set between 350 and 450 per units (p.u.) and the voltage magnitude at first bus is defined as a reference bus, $V_{n_{ref}}^{ref}$=380V.

BUS	V_n^-	V_n^+	P_n^{g-}	P_n^{g+}	$V_{n_{ref}}^{ref}$	SOC_n^-	SOC_n^+	r_n^-	r_n^+
1	-	-	0	10K	380	-	-	-	-
2	350	450	0	10K	-	-	-	-	-
3	350	450	-	-	-	-	-	-	-
4	350	450	-	-	-	-	-	-	-
5	350	450	-	-	-	0.2	0.8	-7K	7K
6	350	450	-	-	-	0.2	0.8	-7K	7K

Table 5.4: The Bound Constraints.

BUS	$\Delta V_{nj}(\kappa)^-$	$\Delta V_{nj}(\kappa)^+$
3 To 4	-2K	2K
4 To 3	-2K	2K
5 To 6	-2K	2K
6 To 5	-2K	2K

Table 5.5: The power capacity constraints

In this scenario, the transmission lines between buses 5 and 6 and between buses 3 and 4 are bounded. The storage battery is bounded by a capacity $SOC_n(\kappa)^-$ and $SOC_n(\kappa)^+$ with a charge or discharge rate (discussed earlier) as $r_n(\kappa)^-$and $r_n(\kappa)^+$. The initial condition of the storage battery was chosen to be 0.7 KWh. A total of 20 KWh of energy was proposed as well as the sampling time of one hour, and the simulations were performed over one day. The simulation results illustrate the advantages of including energy storage devices under low and high demand circumstances.

5.2.8 Demonstration of Scenario-II

The system is illustrated in Fig. 5.6 and includes two storage devices at buses 5 and 6. During the power production, the energy is stored in the battery and released when the $r_n(\kappa)$, value of the power at time (κ), is $r_n(\kappa)^+ \geq 0$ and $r_n(\kappa)^- \leq 0$, respectively.

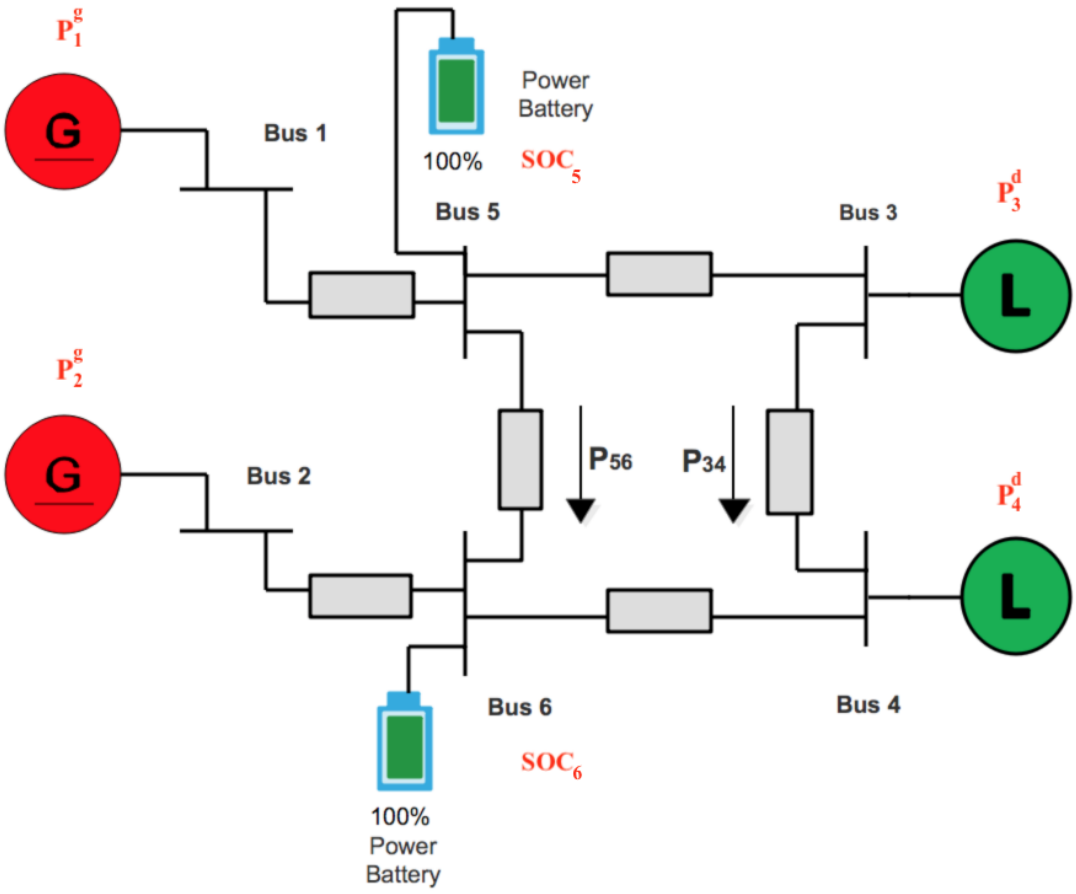

Figure 5.6: Scenario II: A power system with two energy storages.

The following illustration as given earlier: power generations are described by P_n^g, storage power is $r_n(\kappa)$, and the event sampling is α_n. The battery is modeled by its minimum and the maximum values of the energy storage $r_n(\kappa)^-$ and $r_n(\kappa)^+$, and the battery state-of-charge SOC_n, in the range 0.2 and 0.8, this describes energy in this problem.

The optimization problem for this case is:

$$\min_{P_n^g(\kappa), v_n(\kappa), SOC_n(\kappa), r_n(\kappa), U_n(\kappa)} \quad \sum_{\kappa=1}^{24} \left(5P_1^g(\kappa) + 7P_2^g(\kappa)\right) \tag{5.15}$$

subj. to (5.16)

$$380 \leq v_n(\kappa) \leq 450, \quad \forall n \in 6, \quad \kappa \in \tau \tag{5.17}$$

$$0 \leq P_1^g(\kappa) \leq 10K, \quad \kappa \in \tau \tag{5.18}$$

$$0 \leq P_2^g(\kappa) \leq 10K, \quad \kappa \in \tau \tag{5.19}$$

$$-7K \leq r_{[5,6]}(\kappa) \leq 7K, \quad \kappa \in \tau \tag{5.20}$$

$$0.2 \leq SOC_{[5,6]}(\kappa) \leq 0.8, \quad \kappa \in \tau \tag{5.21}$$

$$SOC_{[5,6]}(\kappa + 1) = SOC_{[5,6]}(\kappa) + \alpha_{[5,6]} r_{[5,6]}(\kappa), \kappa \in \tau \tag{5.22}$$

$$P_{[1,2]}^g(\kappa) - P_{[3,4]}^d(\kappa) - r_{[5,6]}(\kappa) = \sum_{j:n\sim j}^{n\in 6} \left\{ v_n(\kappa) - U_{nj}(\kappa) \right\} Y_{nj}, \forall n \in 6, \ \kappa \in \tau \tag{5.23}$$

$$-2K \leq \left\{ v_n(\kappa) - U_{nj}(\kappa) \right\} Y_{nj} \leq 2K \tag{5.24}$$

$$-2K \leq \left\{ v_j(\kappa) - U_{jn}(\kappa) \right\} Y_{jn} \leq 2K \tag{5.25}$$

$$\boldsymbol{R} := \begin{bmatrix} \boldsymbol{M}_{nj} & & \\ & \ddots & \\ & & \boldsymbol{M}_{jn} \end{bmatrix} \geq 0, \quad \forall n \sim j \tag{5.26}$$

- **The Initial Condition (I.C) of $SOC_{[5,6]}$ at $\kappa = 0$**

$$SOC_{[5,6]}(0) = 0.7 \tag{5.27}$$

- **The Voltage Reference at bus n_{ref}**

$$V_{1_{ref}}^{ref}(\kappa) = 380 \tag{5.28}$$

The optimal value of the cost and the running time are shown in Table. 5.6.

Optimal value	1.62046e+06
Computation Time (s)	2.88

Table 5.6: The result of Scenario-II.

The numerical values of power injections and nodal voltages are listed in Appendix-II, Tables 7.5 and 7.6.

5.2.9 System Load Data

Similarly to the previous scenario, the total power load of the DC micro-grids for each hour is shown in Fig. 5.11. This includes the power loads at buses 3 and 4. The power load at bus 3 is constant during the operational time. However, the power load at bus 4 is unsteady with the average hourly power load of around 7.5 kWh.

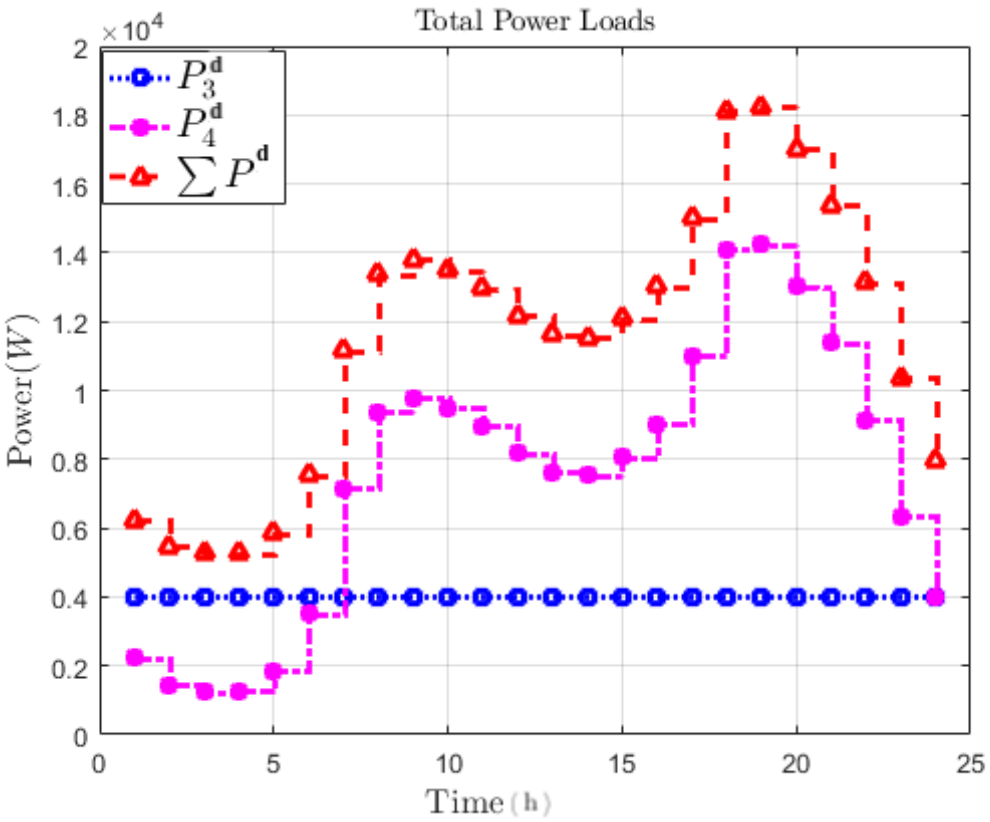

Figure 5.7: The actual power loads

5.2.10 System Generation Data

The power generators schedule for 24 hours is given in Fig. 5.8. In this figure, it can been seen that all generators during the operational time are within the bounds and satisfied the constraints.

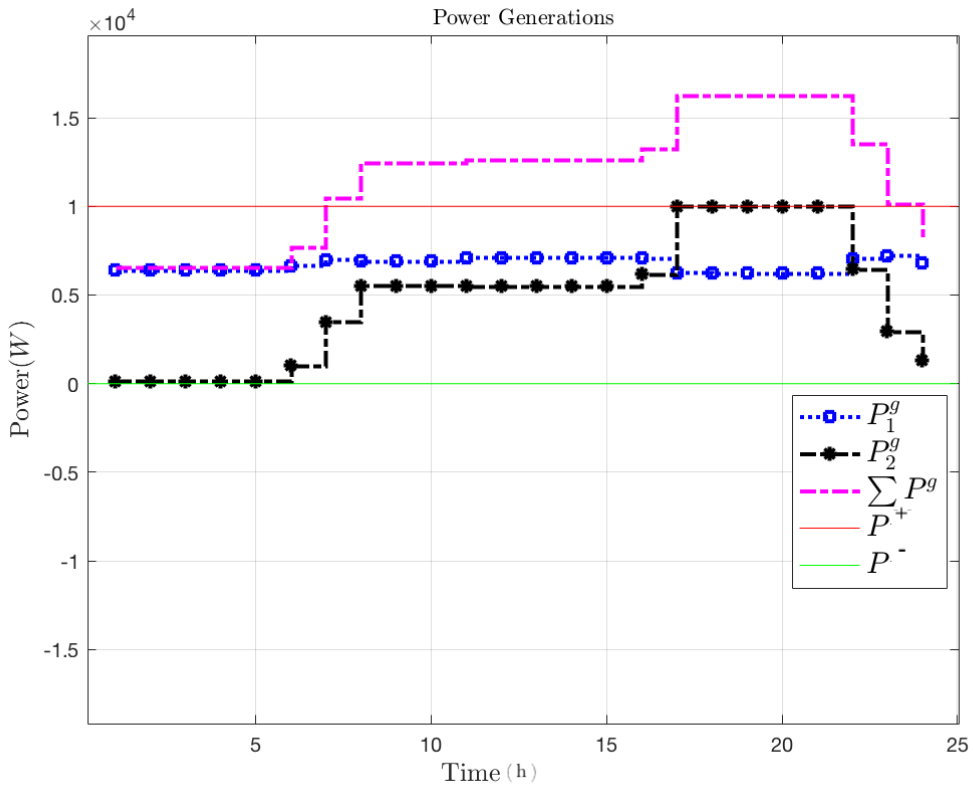

Figure 5.8: The generator schedule

In Fig. 5.9, it can be seen that the battery schedule satisfied the constraints and bounds during the operations. Furthermore, battery charging and discharging happen during the production times as can be seen by noting the graphs. The energy stored in the battery at bus 5 is charging during 1 to 6, 8 to 10, 17 to 18, and between 22 to 23. It is also discharging during at 7, 11 to 16, 18 to 21, and at 24. On the other hand, when the energy at bus 5 is stored in the battery, the battery at bus 6 is discharged from energy. In bus 6 the battery starts to store at the beginning of the operation until hour 7, then it discharges

from hours 8 to 12, then back to restore the battery between 13 and 17, and next the battery discharges during 18 to 22. The stored powers are utilized to feed nearby the loads and avoid losses and the high cost on the system if faraway DC generations feed these loads. Since the battery is not needed to hold any further power at the end of 25 hours, it is economically beneficial to discharge all the battery energy so the net battery energy is 0. The total optimal cost for supplying the load is given in Table. 5.6.

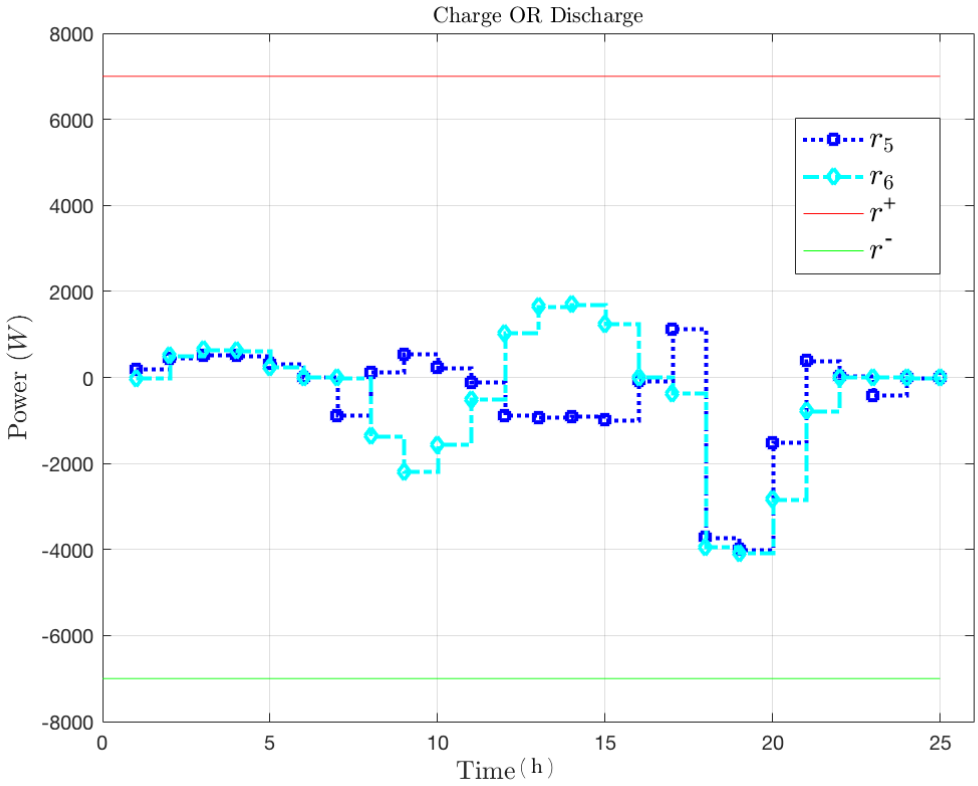

Figure 5.9: The battery schedule

A list of the standby of power battery values are given in Table. 7.6.

5.2.11 State-of-Charge (SOC)

A dynamic OPF problem has been solved due to the dynamics of the state-of-charge (SOC) of the battery. As shown in Fig. 5.10, it can be seen experimentally when the battery is either charged fully SOC = 100% or discharged to SOC = 0%.

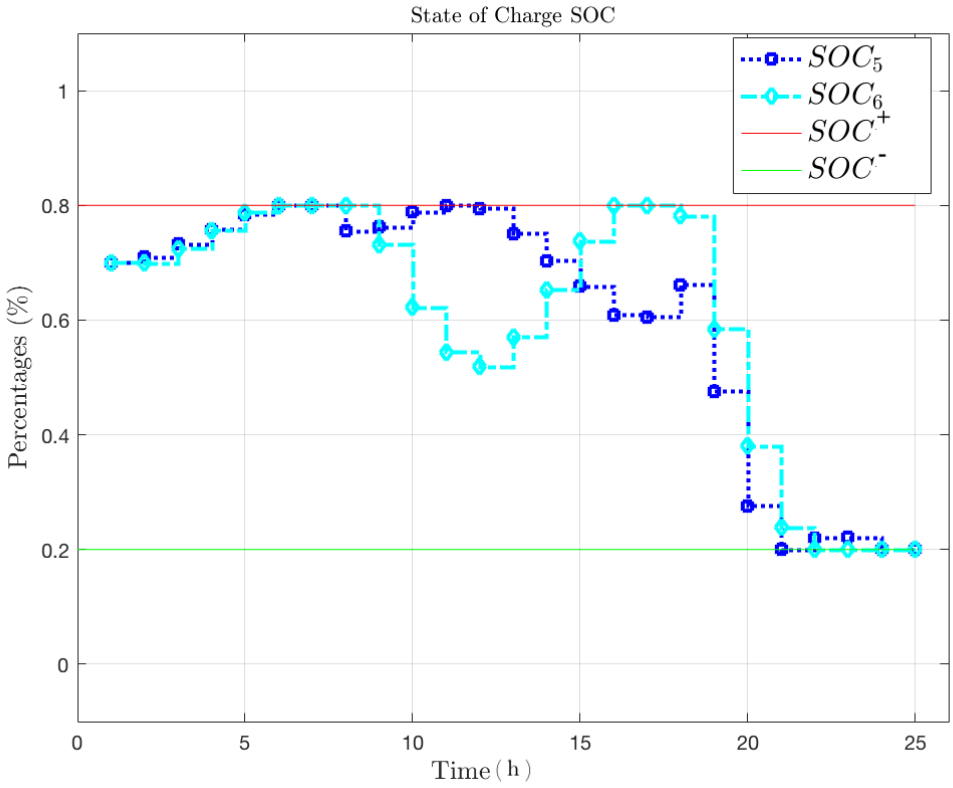

Figure 5.10: The State-of-charge schedule

5.2.12 Analysis of Results

As it can be seen from above scenarios the SOCP is is exact, i.e. $\boldsymbol{Rank(M_{nj})} = 1$ holds, $\forall n \sim j$ and hence the solution found is also a global solution of the original OPF. The scale of the problems solved in this work is small. In practice multi-bus DC systems may integrate a large number of buses. The results of computation time suggests that the proposed method may not be suitable to very large scale systems.

Therefore, following flowchart summarizes the SOPC relaxation approach used to solve the OPF problem.

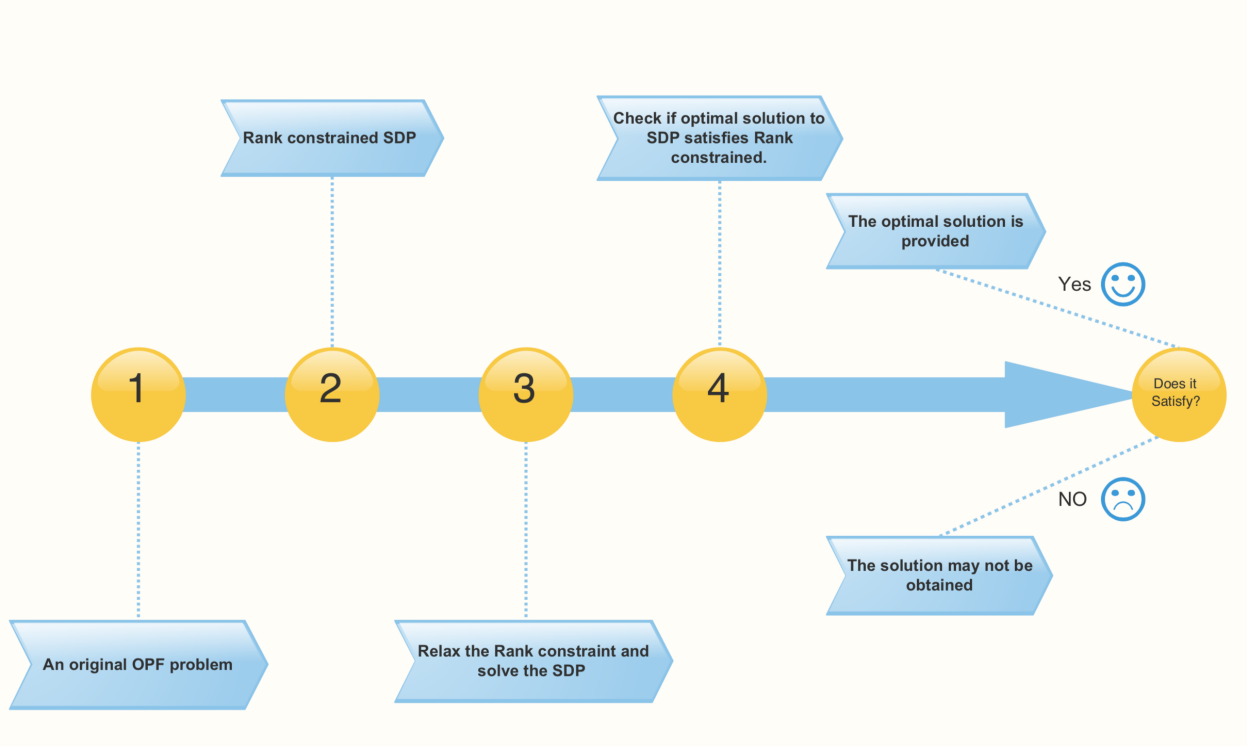

Figure 5.11: The flowchart of the convexification process

The solution of the SOCP includes a set of 2×2 positive semidefinite matrices $M_{nj}, \forall\ n\ j$. Hence it is necessary to check the rank constraint a posteriory. If it is satisfied then the optimal solution is the global solution of the original OPF problem. If it is not satisfied then, in general, nothing can be said [12].

6 | Conclusion and Future Work

6.1 Conclusions

In this work, we formulated an optimal power flow (OPF) problem with dynamic energy storage as a static optimization problem. This results in a nonlinear programming problem. This problem was transformed to a problem with constraints over the cone of positive semidefinite matrices and required the introduction of a rank suitable constraint. The rank constraint was ignored resulting in am SOPC problem which can be solved numerically as using SDP solvers. This approach was tested in various scenarios. One with a single energy storage and another with more energy storage devices.

Analysis of the numerical result analysis of these scenarios shows that the optimal solution is can be obtained, i.e. $\boldsymbol{Rank(M_{nj})} = 1$ holds, $\forall n \sim j$.

Form the figures we can see that, as expected, the energy stored was scheduled to balance the power of loads and generation sources. It can be seen that energy storage provides additional flexibility to the system for handling load variations and power limits, with the potential of providing improved power quality, stability, load following, peak reduction, and reliability.

6.2 Future Work

There are several future research directions that have been revealed as a result of this work. We summarize the most promising below.

- The most important next step is to integrate recent algorithms that explicitly enforce the rank one constraint instead of ignoring it and checking it after the fact. There are a few approaches that can be considered such as the well known nuclear norm minimization [80] and also low-rank inducing norms recently proposed in [81].
- Another research direction to make this practical is necessary to reformulate the problem as a distributed dynamic optimization problem. This will be necessary to solve large-scale power flow problems but will also enable the implementation using low cost embedded system making it more affordable for less affluent and rural communities.
- Finally, it is natural to consider the problem as a polynomial optimization problem given that the nonlinearities are polynomial. This is already happening and will bring powerful alternatives to find global solutions to optimal power flow problems.

7 | APPENDIX

7.1 Appendix-I

Time (hr)	P_3^d	P_4^d
1	4K	2236.89
2	4K	1454.8
3	4K	1248.7
4	4K	1276.1
5	4K	1845.2
6	4K	3523.9
7	4K	7148.9
8	4K	9380.8
9	4K	9794.5
10	4K	9480.1
11	4K	8951.7
12	4K	8178.8
13	4K	7615.9
14	4K	7543.5
15	4K	8071.9
16	4K	9013.8
17	4K	11005
18	4K	14109
19	4K	14249
20	4K	13005
21	4K	11393
22	4K	9145.9
23	4K	6354.0
24	4K	3973.6

Table 7.1: Power Load for Scenario-I.

Time (hours)	P_1^g	P_2^g	$\sum P^g$
1	6214.7	142.84	6357.6
2	5942.3	143.11	6085.4
3	5870.6	143.18	6013.7
4	5880.1	143.17	6023.3
5	6078.2	142.96	6221.2
6	6664.4	10222	7686.4
7	7939.4	3481.2	11421
8	6781.5	5536.1	12318
9	6347.5	5553.8	11901
10	6677.2	5540.3	12218
11	7233.0	5517.7	12751
12	8050.1	5484.4	13535
13	8104.6	5482.0	13587
14	8079	5483	13562
15	8163.4	5479.8	13643
16	7167.6	6170	13338
17	6221.4	10K	16221
18	8492.4	10K	18492
19	8790.1	10K	18790
20	7940.7	10K	17941
21	7932.2	10K	17932
22	7028.5	6446.3	13475
23	7658.7	2938.1	10597
24	6821.9	1324.6	8146.5

Table 7.2: Power Generation for Scenario-I.

Time (hr)	P_3^{Loads}	P_4^{Loads}	$\sum P^{\text{Loads}}$	r_6
1	4K	2236.89	6236.9	-16.810
2	4K	1454.8	5454.8	505.15
3	4K	1248.7	5248.7	642.67
4	4K	1276.1	5276.1	624.39
5	4K	1845.2	5845.2	244.60
6	4K	3523.9	7523.9	1.5456e-04
7	4K	7148.9	11149	-2.6321e-05
8	4K	9380.8	13381	-1343.2
9	4K	9794.5	13795	-2154.7
10	4K	9480.1	13480	-1538.0
11	4K	8951.7	12952	-501.96
12	4K	8178.8	12179	1013.3
13	4K	7615.9	11616	1626.3
14	4K	7543.5	11544	1675.6
15	4K	8071.9	12072	1222.8
16	4K	9013.8	13014	3.5765e-04
17	4K	11005	15005	-5.6655e-05
18	4K	14109	18109	-4473.9
19	4K	14249	18249	-4614.8
20	4K	13005	17005	-2801.1
21	4K	11393	15393	-110.20
22	4K	9145.9	13146	6.7061e-05
23	4K	6354.0	10354	7.3379e-05
24	4K	3973.6	7973.6	-1.4010e-04

Table 7.3: Power Load and rate of charge for Scenario-I.

7.2 Appendix-II

Time (hr)	P_3^d	P_4^d
1	4K	2236.89
2	4K	1454.8
3	4K	1248.7
4	4K	1276.1
5	4K	1845.2
6	4K	3523.9
7	4K	7148.9
8	4K	9380.8
9	4K	9794.5
10	4K	9480.1
11	4K	8951.7
12	4K	8178.8
13	4K	7615.9
14	4K	7543.5
15	4K	8071.9
16	4K	9013.8
17	4K	11005
18	4K	14109
19	4K	14249
20	4K	13005
21	4K	11393
22	4K	9145.9
23	4K	6354.0
24	4K	3973.6

Table 7.4: Power Load for Scenario-II.

Time (hr)	P_1^g	P_2^g	$\sum P^g$
1	6414.5	143.05	6557.5
2	6415.2	143.05	6558.2
3	6415.4	143.05	6558.4
4	6415.4	143.06	6558.4
5	6415	143.07	6558
6	6664.4	1022	7686.4
7	7004.9	3480.9	10486
8	6912.4	5515.5	12428
9	6911	5516.2	12427
10	6912.2	5515.7	12428
11	7118.8	5506.7	12625
12	7121	5505.4	12626
13	7122.7	5505	12628
14	7122.8	5505	12628
15	7121.3	5505.2	12627
16	7082.7	6169.9	13253
17	6261.6	10K	16262
18	6222.8	10K	16223
19	62208	10K	16221
20	6237.8	10K	16238
21	6245.9	10K	16246
22	7054.6	6446.3	13501
23	7216.7	2938	10155
24	6821.8	1324.6	8146.5

Table 7.5: Power Generation for Scenario-II.

Time (hr)	P_3^{Loads}	P_4^{Loads}	$\sum P^{L\text{Loads}}$	r_5	r_6	$r_5 + r_6$
1	4K	2236.89	6236.9	191.00	-16.598	174.40
2	4K	1454.8	5454.8	452.67	505.08	957.75
3	4K	1248.7	5248.7	521.61	642.54	1164.1
4	4K	1276.1	5276.1	512.48	624.27	1136.8
5	4K	1845.2	5845.2	322.21	244.71	566.91
6	4K	3523.9	7523.9	8.3177e-03	3.2036e-03	1.1521e-02
7	4K	7148.9	11149	-886.16	-4.1974e-04	-886.16
8	4K	9380.8	13381	124.65	-1363.2	-1238.5
9	4K	9794.5	13795	537.59	-2191.4	-1653.8
10	4K	9480.1	13480	223.91	-1562	-1338.1
11	4K	8951.7	12952	-108.55	-512.41	-620.95
12	4K	8178.8	12179	-880.24	1034.2	153.97
13	4K	7615.9	11616	-930.12	1649.2	719.05
14	4K	7543.5	11544	-905.76	1697.5	791.74
15	4K	8071.9	12072	-986.95	1248.0	261.05
16	4K	9013.8	13014	-80.645	6.8607e-03	-80.639
17	4K	11005	15005	1129.4	-363.74	765.62
18	4K	14109	18109	-3720.4	-3946.0	-7666.4
19	4K	14249	18249	-3998.7	-4087.3	-8086.0
20	4K	13005	17005	-1517.5	-2831.0	-4348.4
21	4K	11393	15393	393.90	-772.0	-378.10
22	4K	9145.9	13146	24.843	1.2644e-03	24.844
23	4K	6354.0	10354	-419.24	1.4531e-03	-419.24
24	4K	3973.6	7973.6	-1.3429e-02	-2.7123e-03	-1.6141e-02

Table 7.6: Power Load and rate of charge for Scenario-II.

Bibliography

[1] T. Markvart, *Solar electricity*, vol. 6. John Wiley & Sons, 2000.

[2] B. Parida, S. Iniyan, and R. Goic, "A review of solar photovoltaic technologies," *Renewable and sustainable energy reviews*, vol. 15, no. 3, pp. 1625–1636, 2011.

[3] G. K. Singh, "Solar power generation by PV (photovoltaic) technology: A review," *Energy*, vol. 53, pp. 1–13, 2013.

[4] T. Ackermann, G. Andersson, and L. Söder, "Distributed generation: a definition," *Electric power systems research*, vol. 57, no. 3, pp. 195–204, 2001.

[5] M. Barnes, J. Kondoh, H. Asano, J. Oyarzabal, G. Ventakaramanan, R. Lasseter, N. Hatziargyriou, and T. Green, "Real-world microgrids-an overview," in *System of Systems Engineering, 2007. SoSE'07. IEEE International Conference on*, pp. 1–8, IEEE, 2007.

[6] N. Pogaku, M. Prodanovic, and T. C. Green, "Modeling, analysis and testing of autonomous operation of an inverter-based microgrid," *IEEE Transactions on power electronics*, vol. 22, no. 2, pp. 613–625, 2007.

[7] O. Palizban and K. Kauhaniemi, "Energy storage systems in modern grids—matrix of technologies and applications," *Journal of Energy Storage*, vol. 6, pp. 248–259, 2016.

[8] H. Chen, T. N. Cong, W. Yang, C. Tan, Y. Li, and Y. Ding, "Progress in electrical energy storage system: A critical review," *Progress in Natural Science*, vol. 19, no. 3, pp. 291–312, 2009.

[9] S. Abu-Sharkh, R. Arnold, J. Kohler, R. Li, T. Markvart, J. Ross, K. Steemers, P. Wilson, and R. Yao, "Can microgrids make a major contribution to UK energy supply?," *Renewable and Sustainable Energy Reviews*, vol. 10, no. 2, pp. 78–127, 2006.

[10] M. Basu, "Economic environmental dispatch using multi-objective differential evolution," *Applied soft computing*, vol. 11, no. 2, pp. 2845–2853, 2011.

[11] N. Kok, N. Miller, and P. Morris, "The economics of green retrofits," *Journal of Sustainable Real Estate*, vol. 4, no. 1, pp. 4–22, 2012.

[12] S. H. Low, "Convex relaxation of optimal power flow—part i: Formulations and equivalence," *IEEE Transactions on Control of Network Systems*, vol. 1, no. 1, pp. 15–27, 2014.

[13] D. Salomonsson, L. Soder, and A. Sannino, "An adaptive control system for a DC microgrid for data centers," in *Industry Applications Conference, 2007. 42nd IAS Annual Meeting. Conference Record of the 2007 IEEE*, pp. 2414–2421, IEEE, 2007.

[14] H. Kakigano, Y. Miura, and T. Ise, "Low-voltage bipolar-type DC microgrid for super high quality distribution," *IEEE transactions on power electronics*, vol. 25, no. 12, pp. 3066–3075, 2010.

[15] C.-C. Lin, H. Peng, J. W. Grizzle, and J.-M. Kang, "Power management strategy for a parallel hybrid electric truck," *IEEE transactions on control systems technology*, vol. 11, no. 6, pp. 839–849, 2003.

[16] K. Divya and J. Østergaard, "Battery energy storage technology for power systems—an overview," *Electric Power Systems Research*, vol. 79, no. 4, pp. 511–520, 2009.

[17] C. W. Gellings, *The smart grid: enabling energy efficiency and demand response*. The Fairmont Press, Inc., 2009.

[18] J. M. Guerrero, L. Hang, and J. Uceda, "Control of distributed uninterruptible power supply systems," *IEEE Transactions on Industrial Electronics*, vol. 55, no. 8, pp. 2845–2859, 2008.

[19] J. M. Guerrero, J. C. Vasquez, J. Matas, L. G. De Vicuña, and M. Castilla, "Hierarchical control of droop-controlled AC and DC microgrids — a general approach toward standardization," *IEEE Transactions on industrial electronics*, vol. 58, no. 1, pp. 158–172, 2011.

[20] J. Li, F. Liu, Z. Wang, S. H. Low, and S. Mei, "Optimal power flow in stand-alone DC microgrids," *arXiv preprint arXiv:1708.05140*, 2017.

[21] J. Carpentier, "Contribution to the economic dispatch problem," *Bulletin de la Societe Francoise des Electriciens*, vol. 3, no. 8, pp. 431–447, 1962.

[22] L. Gan and S. H. Low, "Optimal power flow in direct current networks," *IEEE Transactions on Power Systems*, vol. 29, no. 6, pp. 2892–2904, 2014.

[23] O. Alsac, J. Bright, M. Prais, and B. Stott, "Further developments in LP-based optimal power flow," *IEEE Transactions on Power Systems*, vol. 5, no. 3, pp. 697–711, 1990.

[24] J. A. Momoh, R. Adapa, and M. El-Hawary, "A review of selected optimal power flow literature to 1993. i. nonlinear and quadratic programming approaches," *IEEE transactions on power systems*, vol. 14, no. 1, pp. 96–104, 1999.

[25] F. Capitanescu and L. Wehenkel, "A new iterative approach to the corrective security-constrained optimal power flow problem," *IEEE transactions on power systems*, vol. 23, no. 4, pp. 1533–1541, 2008.

[26] P. E. Onate and J. M. Ramirez, "Optimal power flow including transient stability constraints," in *Transmission and Distribution Conference and Exposition, 2008. T&D. IEEE/PES*, pp. 1–9, IEEE, 2008.

[27] B. Stott and E. Hobson, "Power system security control calculations using linear programming, part i," *IEEE Transactions on Power Apparatus and Systems*, no. 5, pp. 1713–1720, 1978.

[28] S. Sojoudi and J. Lavaei, "Physics of power networks makes hard optimization problems easy to solve," in *Power and Energy Society General Meeting, 2012 IEEE*, pp. 1–8, IEEE, 2012.

[29] R. Madani, S. Sojoudi, and J. Lavaei, "Convex relaxation for optimal power flow problem: Mesh networks," *IEEE Transactions on Power Systems*, vol. 30, no. 1, pp. 199–211, 2015.

[30] J. A. Momoh, M. El-Hawary, and R. Adapa, "A review of selected optimal power flow literature to 1993. ii. newton, linear programming and interior point methods," *IEEE Transactions on Power Systems*, vol. 14, no. 1, pp. 105–111, 1999.

[31] J. T. Betts, *Practical methods for optimal control and estimation using nonlinear programming*. SIAM, 2010.

[32] X. Bai, H. Wei, K. Fujisawa, and Y. Wang, "Semidefinite programming for optimal power flow problems," *International Journal of Electrical Power & Energy Systems*, vol. 30, no. 6, pp. 383–392, 2008.

[33] X. Bai and H. Wei, "Semi-definite programming-based method for security-constrained unit commitment with operational and optimal power flow constraints," *IET Generation, Transmission & Distribution*, vol. 3, no. 2, pp. 182–197, 2009.

[34] J. Lavaei and S. H. Low, "Zero duality gap in optimal power flow problem," *IEEE Transactions on Power Systems*, vol. 27, no. 1, pp. 92–107, 2012.

[35] Z. Wang, F. Liu, Y. Chen, S. H. Low, and S. Mei, "Unified distributed control of stand-alone DC microgrids," *IEEE Transactions on Smart Grid*, 2017.

[36] S. Kim and M. Kojima, "Exact solutions of some nonconvex quadratic optimization problems via sdp and socp relaxations," *Computational Optimization and Applications*, vol. 26, no. 2, pp. 143–154, 2003.

[37] G. Andersson, "Power system analysis," *Eidgenössische Technische Hochschule Zürich (ETH)*, 2011.

[38] S. Frank, I. Steponavice, and S. Rebennack, "Optimal power flow: a bibliographic survey i," *Energy Systems*, vol. 3, no. 3, pp. 221–258, 2012.

[39] P. Kundur, N. J. Balu, and M. G. Lauby, *Power system stability and control*, vol. 7. McGraw-hill New York, 1994.

[40] W. Zhang, F. Li, and L. M. Tolbert, "Review of reactive power planning: objectives, constraints, and algorithms," *IEEE transactions on power systems*, vol. 22, no. 4, pp. 2177–2186, 2007.

[41] Q. Jiang, H.-D. Chiang, C. Guo, and Y. Cao, "Power–current hybrid rectangular formulation for interior-point optimal power flow," *IET generation, transmission & distribution*, vol. 3, no. 8, pp. 748–756, 2009.

[42] M. Abido, "Optimal power flow using particle swarm optimization," *International Journal of Electrical Power & Energy Systems*, vol. 24, no. 7, pp. 563–571, 2002.

[43] M. Modiri-Delshad, S. Koohi-Kamali, E. Taslimi, S. H. A. Kaboli, and N. Rahim, "Economic dispatch in a microgrid through an iterated-based algorithm," in *Clean Energy and Technology (CEAT), 2013 IEEE Conference on*, pp. 82–87, IEEE, 2013.

[44] H. Bouchekara, M. Abido, and M. Boucherma, "Optimal power flow using teaching-learning-based optimization technique," *Electric Power Systems Research*, vol. 114, pp. 49–59, 2014.

[45] I. Farhat and M. El-Hawary, "Optimization methods applied for solving the short-term hydrothermal coordination problem," *Electric Power Systems Research*, vol. 79, no. 9, pp. 1308–1320, 2009.

[46] P. Gill, *Electrical power equipment maintenance and testing*. CRC press, 2008.

[47] K. Pandya and S. Joshi, "A survey of optimal power flow methods.," *Journal of Theoretical & Applied Information Technology*, vol. 4, no. 5, 2008.

[48] J. Momoh, R. Koessler, M. Bond, B. Stott, D. Sun, A. Papalexopoulos, and P. Ristanovic, "Challenges to optimal power flow," *IEEE Transactions on Power Systems*, vol. 12, no. 1, pp. 444–455, 1997.

[49] H. Wang and R. J. Thomas, "Towards reliable computation of large-scale market-based optimal power flow," in *System Sciences, 2007. HICSS 2007. 40th Annual Hawaii International Conference on*, pp. 117–117, IEEE, 2007.

[50] J. M. Carrasco, L. G. Franquelo, J. T. Bialasiewicz, E. Galván, R. C. PortilloGuisado, M. M. Prats, J. I. León, and N. Moreno-Alfonso, "Power-electronic systems for the grid integration of renewable energy sources: A survey," *IEEE Transactions on industrial electronics*, vol. 53, no. 4, pp. 1002–1016, 2006.

[51] B. Stott and E. Hobson, "Power system security control calculations using linear programming, part ii," *IEEE Transactions on Power Apparatus and Systems*, no. 5, pp. 1721–1731, 1978.

[52] R. E. Griffith and R. Stewart, "A nonlinear programming technique for the optimization of continuous processing systems," *Management science*, vol. 7, no. 4, pp. 379–392, 1961.

[53] X.-P. Zhang, C. Rehtanz, and B. Pal, *Flexible AC transmission systems: modelling and control*. Springer Science & Business Media, 2012.

[54] R. Mota-Palomino and V. Quintana, "Sparse reactive power scheduling by a penalty function-linear programming technique," *IEEE Transactions on Power Systems*, vol. 1, no. 3, pp. 31–39, 1986.

[55] O. Mangasarian, "Nonlinear programming: Sequential unconstrained minimization techniques (Anthony V. Fiacco and Garth P. McCormick)," *SIAM Review*, vol. 12, no. 4, p. 593, 1970.

[56] R. Burchett, H. Happ, and K. Wirgau, "Large scale optimal power flow," *IEEE Transactions on Power Apparatus and Systems*, no. 10, pp. 3722–3732, 1982.

[57] X. Lin, A. David, and C. Yu, "Reactive power optimisation with voltage stability consideration in power market systems," *IEE Proceedings-Generation, Transmission and Distribution*, vol. 150, no. 3, pp. 305–310, 2003.

[58] G. Granelli and M. Montagna, "Security-constrained economic dispatch using dual quadratic programming," *Electric Power Systems Research*, vol. 56, no. 1, pp. 71–80, 2000.

[59] H. W. Dommel and W. F. Tinney, "Optimal power flow solutions," *IEEE Transactions on power apparatus and systems*, no. 10, pp. 1866–1876, 1968.

[60] R. Burchett, H. H. Happ, D. Vierath, and K. Wirgau, "Developments in optimal power flow," *IEEE Transactions on Power Apparatus and Systems*, no. 2, pp. 406–414, 1982.

[61] E. P. De Carvalho, A. dos Santos Junior, and T. F. Ma, "Reduced gradient method combined with augmented lagrangian and barrier for the optimal power flow problem," *Applied Mathematics and Computation*, vol. 200, no. 2, pp. 529–536, 2008.

[62] J. Peschon, D. W. Bree, and L. P. Hajdu, "Optimal power-flow solutions for power system planning," *Proceedings of the IEEE*, vol. 60, no. 1, pp. 64–70, 1972.

[63] A. Sasson, F. Viloria, and F. Aboytes, "Optimal load flow solution using the hessian matrix," *IEEE Transactions on Power Apparatus and Systems*, no. 1, pp. 31–41, 1973.

[64] H. Happ, "Optimal power dispatch a comprehensive survey," *IEEE Transactions on Power Apparatus and Systems*, vol. 96, no. 3, pp. 841–854, 1977.

[65] G. Da Costa, C. Costa, and A. De Souza, "Comparative studies of optimization methods for the optimal power flow problem," *Electric Power Systems Research*, vol. 56, no. 3, pp. 249–254, 2000.

[66] J. Nocedal and S. Wright, *Numerical Optimization*. Springer, 2006.

[67] R. A. Jabr, "A primal-dual interior-point method to solve the optimal power flow dispatching problem," *Optimization and Engineering*, vol. 4, no. 4, pp. 309–336, 2003.

[68] G. L. Torres and V. H. Quintana, "An interior-point method for nonlinear optimal power flow using voltage rectangular coordinates," *IEEE transactions on Power Systems*, vol. 13, no. 4, pp. 1211–1218, 1998.

[69] G. L. Torres and V. H. Quintana, "On a nonlinear multiple-centrality-corrections interior-point method for optimal power flow," *IEEE Transactions on Power Systems*, vol. 16, no. 2, pp. 222–228, 2001.

[70] K. Karoui, L. Platbrood, H. Crisciu, and R. A. Waltz, "New large-scale security constrained optimal power flow program using a new interior point algorithm," in *Elec-*

tricity Market, 2008. EEM 2008. 5th International Conference on European, pp. 1–6, IEEE, 2008.

[71] S. Granville, J. Mello, and A. Melo, "Application of interior point methods to power flow unsolvability," *IEEE Transactions on Power Systems*, vol. 11, no. 2, pp. 1096–1103, 1996.

[72] A. El-Bakry, R. A. Tapia, T. Tsuchiya, and Y. Zhang, "On the formulation and theory of the newton interior-point method for nonlinear programming," *Journal of Optimization Theory and Applications*, vol. 89, no. 3, pp. 507–541, 1996.

[73] X. Zhang, S. Petoussis, and K. Godfrey, "Nonlinear interior-point optimal power flow method based on a current mismatch formulation," *IEE Proceedings-Generation, Transmission and Distribution*, vol. 152, no. 6, pp. 795–805, 2005.

[74] J. Lavaei, "Zero duality gap for classical opf problem convexifies fundamental nonlinear power problems," in *American Control Conference (ACC), 2011*, pp. 4566–4573, IEEE, 2011.

[75] J. Zhang, "On distributed optimization methods for solving optimal power flow problem over electricity grids," 2016.

[76] X. Yao, "Study on DC arc faults in ring-bus DC microgrids with constant power loads," in *Energy Conversion Congress and Exposition (ECCE), 2016 IEEE*, pp. 1–5, IEEE, 2016.

[77] M. Grant and S. Boyd, "CVX: Matlab software for disciplined convex programming, version 2.1." `http://cvxr.com/cvx`, Mar. 2014.

[78] M. Grant and S. Boyd, "Graph implementations for nonsmooth convex programs," in *Recent Advances in Learning and Control* (V. Blondel, S. Boyd, and H. Kimura, eds.),

Lecture Notes in Control and Information Sciences, pp. 95–110, Springer-Verlag Limited, 2008. http://stanford.edu/~boyd/papers/graph_dcp.html.

[79] K. M. Chandy, S. H. Low, U. Topcu, and H. Xu, "A simple optimal power flow model with energy storage," in *Decision and Control (CDC), 2010 49th IEEE Conference on*, pp. 1051–1057, IEEE, 2010.

[80] B. Recht, M. Fazel, and P. A. Parrilo, "Guaranteed minimum-rank solutions of linear matrix equations via nuclear norm minimization," *SIAM review*, vol. 52, no. 3, pp. 471–501, 2010.

[81] C. Grussler and P. Giselsson, "Low-rank inducing norms with optimality interpretations," *arXiv preprint arXiv:1612.03186*, 2016.